Opsonic phagocytosis in chronic obstructive pulmonary disease is enhanced by Nrf2 agonists.

Martin A. Bewley[1], Richard C Budd[1,2], Eilise Ryan[3], Joby Cole[1,2], Paul Collini[1,2], Jennifer Marshall[3], Umme Kolsum[4], Gussie Beech[4], Richard D. Emes[5], Irina Tcherniaeva[6], Guy A. M. Berbers[6], Sarah R. Walmsley[3], Gavin Donaldson[7], Jadwiga A. Wedzicha[7,] Iain Kilty[8], William Rumsey[9], Yolanda Sanchez[9], Christopher E. Brightling[10], Louise E. Donnelly[7], Peter J. Barnes[7], Dave Singh[4], Moira K.B. Whyte[3] and David H. Dockrell[11]* on behalf of COPDMAP.

[1] Department of Infection Immunity and Cardiovascular Disease and The Florey Institute for Host-Pathogen Interactions, University of Sheffield Medical School, UK, [2]Sheffield Teaching Hospitals, [3]Department of Respiratory Medicine and MRC Centre for Inflammation Research, University of Edinburgh, [4]Medicines Evaluation Unit, University of Manchester and University Hospital of South Manchester, [5] School of Veterinary Medicine and Science and Advanced Data Analysis Centre, University of Nottingham, UK, [6] Center for Infectious Disease Control (CIb), National Institute for Public Health and the Environment (RIVM), Utrecht, the Netherlands, [7]National Heart and Lung Institute, University of London Imperial College, UK, [8] Pfizer Inc, Cambridge, Massachusetts,[9] Stress and Repair Discovery Performance Unit, Respiratory Therapy Area, GSK, King of Prussia, USA [10]Institute for Lung Health, University of Leicester, UK , [11]Department of Infection Medicine and MRC Centre for Inflammation Research, University of Edinburgh. **Corresponding Author:** David H. Dockrell, The MRC/University of Edinburgh Centre for Inflammation Research, 47 Little France Crescent, Edinburgh, Edinburgh EH16 4TJ UK Phone: +44 (0) 131 242 658 Fax: +44 (0) 131 242 6578 email: david.dockrell@ed.ac.uk.

Author contributions: MAB, ER performed killing assays, flow cytometry, microscopy and collected data. MAB and JC produced figures. RCB, ER, UK, PC and DS co-ordinated and performed bronchoscopies to obtain patient samples. RCB, UK and GB performed clinical phenotyping. JC, ER and RE performed transcriptomic analysis. IT and GB provided multiplex immunoassays on BAL, WR and YS provided compounds and input into experimental design. GD, JAW, SRW, IK, LED, PJB, DS and CEB co-ordinated collection of the COPD patient cohort and controls, shared expertise in assays and provided reagents. MAB, MKBW and DHD designed

and conceived the experiments. MAB, MKW and DHD wrote the manuscript with input from all other authors.

This research was funded by the Medical Research Council (MRC) and the Association of the British Pharmaceutical Industry (ABPI) though support for the COPD-MAP consortium.

Running title: Nrf2 enhances opsonic phagocytosis in COPD.
Descriptor Number: 10.9 Pathogen/Host cell interactions (9.13 COPD pathogenesis, 9.14 COPD pharmacological treatment)
Abstract 250 Total word count: 3,708
At a glance summary:
Scientific Knowledge on the Subject: COPD macrophages have defective phagocytosis but the mechanism and clinical relevance remain unknown.
What This Study Adds to the Field: COPD alveolar macrophages (AM) have a specific defect in opsonic phagocytosis which correlates with clinical phenotype. COPD AM fail to engage an anti-oxidant transcriptional module following exposure to opsonized bacteria. Agonists of a key transcriptional regulator of anti-oxidant host defense, Nrf2, reverse the opsonic phagocytosis defect in COPD and offer a potential therapeutic approach to correct the defect.

Footnote:
Presented in part as "COPD alveolar macrophages have a defect in opsonic phagocytosis of serotype 14 *Streptococcus pneumoniae*". M.Bewley, R.Budd, D.Singh, P.J. Barnes, L.E. Donnelly, D.H.Dockrell and M.K.Whyte. American Thoracic Society International Conference San Diego May 18th, 2014. Am J. Respir Crit Care Med 189:2014; A1011

This article has an online data supplement, which is accessible from this issue's table of content online at **www.atsjournals.org**

Abstract

Rationale: Previous studies have identified defects in bacterial phagocytosis by alveolar macrophages (AM) in patients with chronic obstructive pulmonary disease (COPD) but the mechanisms and clinical consequences remain incompletely defined.

Objectives: To examine the effect of COPD on AM phagocytic responses and identify the mechanisms, clinical consequences and potential for therapeutic manipulation of these defects.

Methods: We isolated alveolar macrophages (AM) and monocyte-derived macrophages (MDM) from a cohort of COPD patients and controls within the MRC COPD-MAP consortium and measured phagocytosis of bacteria in relation to opsonic conditions and clinical features.

Measurements and Main Results: COPD AM and MDM have impaired phagocytosis of *S. pneumoniae*. COPD AM have a selective defect in uptake of opsonized bacteria, despite the presence of anti-pneumococcal antibodies in bronchoalveolar lavage, not observed in MDM or healthy donor's AM. AM defects in phagocytosis in COPD are significantly associated with exacerbation frequency, isolation of pathogenic bacteria and health related quality of life scores. Bacterial binding and initial intracellular killing of opsonized bacteria in COPD AM was not reduced. COPD AM have reduced transcriptional responses to opsonized bacteria, including cellular stress responses that include transcriptional modules involving antioxidant defenses and Nrf2-regualted genes. Agonists of the cytoprotective transcription factor Nrf2 (sulforaphane and Compound 7) reverse defects in phagocytosis of *S. pneumoniae* and non-type able *Haemophilus influenzae* by COPD AM.

Conclusions: Patients with COPD have clinically relevant defects in opsonic

phagocytosis by AM, associated with impaired transcriptional responses to cellular stress, which are reversed by therapeutic targeting with Nrf2 agonists.

Introduction.

Chronic Obstructive Pulmonary Disease (COPD) is a chronic inflammatory lung condition characterised by progressive airflow limitation (1, 2). COPD is associated with increased susceptibility to bacterial airway infection. Exacerbations cause acute worsening of symptoms, leading to hospitalization (3) and to disease progression (4). Approximately 50% of exacerbations are due to bacterial infection (5) and, in a long-term cohort study, the lower airways were chronically colonized with S*treptococcus pneumoniae* in a third of patients (6). Individuals living with COPD are also at increased risk of community-acquired pneumonia (CAP) with increased mortality, most often caused by *S. pneumoniae* (7). This suggests COPD leads to an innate immune defect against *S. pneumoniae* and other bacteria.

Alveolar macrophages (AM) are the resident phagocytes enabling bacterial clearance from the lung, but COPD AM demonstrate reduced phagocytosis of *Haemophilus influenzae* and *P. aeruginosa* (8, 9), while COPD monocyte-derived macrophages (MDM) show impaired phagocytosis of *S. pneumoniae* (10). Bacterial phagocytosis by macrophages involves both non-opsonic and opsonic pathways (11, 12). Previous studies of COPD macrophages have examined non-opsonic or complement-mediated phagocytosis but phagocytosis in the presence of opsonizing antibody has not been studied in detail. A specific defect in opsonic phagocytosis would be particularly relevant to capsulated micro-organisms, such as *S. pneumoniae,* which require opsonization for efficient phagocytosis (13), involving both IgG and complement present in alveolar fluid (14).

We investigated mechanisms underlying phagocytic defects in the COPD lung. COPD Opsonization fails to enhance AM phagocytosis, although it enhances MDM phagocytosis. The level of AM opsonic phagocytosis was strongly associated with clinical and microbiological phenotype. AM responses to opsonized *S. pneumoniae* activated cellular stress transcriptional responses to antioxidant responses, but these were abrogated in COPD AM. Agonists of the antioxidant transcription factor, nuclear factor (erythroid-derived2) like 2 (NFE2L2) or Nrf2, a prominent component of antioxidant transcriptional responses, corrected the defect in AM opsonic phagocytosis in COPD. Some of the results of these studies have been previously reported in the form of an abstract (15).

Methods

Macrophage donors: COPD patients, free from exacerbation, were recruited from the UK Medical Research Council (MRC) COPD-MAP consortium with written approved consent, as outlined online.

Cells and Infection: AM were isolated from broncho-alveolar lavage (BAL) as previously described (13). Cells were >95% AM as assessed by Diff-Quick staining (Dade Behring) visualised by light microscopy (Leica DMRB 1000). Human MDM were differentiated for 14 d from peripheral blood mononuclear cells isolated from donors with written informed consent by Percoll (Sigma) gradient. Cells were cultured in RPMI (Lonza) supplemented with 10% FCS with low LPS (Lonza). Some cells were incubated with 10 μM of sulforaphane, 0.065 μM Compound 7, a selective inhibitor of the Kelch-like ECH-associated protein 1 (KEAP1) /Nrf-2 interaction (16), or vehicle control for 16 h before challenge with bacteria.

Bacteria: Serotype 14 *S. pneumoniae* (NCTC11902) represents a serotype commonly causing infection in COPD (17). Stocks were grown as previously described (18). Non-typeable *H. influenzae (*NCTC 1269) was cultured as outlined in the online supplement. Macrophages were infected at a multiplicity of infection (MOI) of 10:1. *S. pneumoniae* were opsonized for 15 min. with immune serum obtained from volunteers vaccinated with pneumococcal polysaccharide vaccine, and with detectable antibody levels against *S. pneumoniae*, prior to macrophage challenge (13). Viable intracellular bacteria were measured at 4 h post-challenge as a measure of bacterial internalization using a gentamicin protection assay (GPA) as previously described (19). For assessment of early *S. pneumoniae* killing, macrophages were challenged for

4 h before GPA, while additional wells were placed in media containing 0.75 μg/ml vancomycin before GPA at the designated time points.

Bacterial binding: Bacterial binding and internalisation were assessed by fluorescence microscopy (Leica DMRB 1000) (13). Detailed information can be found in the online supplement.

Cell surface marker expression. Cell surface marker expression was measured by flow cytometry, as described online.

Transcriptomic analysis: RNA was extracted and hybridized onto the Affymetrix HG-U133 plus 2.0 Array. Data were analysed in R using affyPML and Limma. Enrichment analysis of Gene Ontology (GO) terms using a Hypergeometric model using GOstats package in R was performed for differentially expressed genes. False discovery rates (FDR) were corrected with the Benjamini-Hochberg procedure. More detailed information is included in the online supplement.

Western blot: Whole cell extracts were isolated using SDS-lysis buffer and separated by SDS gel electrophoresis, as described in the online supplement.

Statistics: Results are recorded as mean and SEM. Sample sizes were informed by standard errors obtained from similar assays in prior publications (13, 18). Decisions on use of parametric or non-parametric tests were based upon results of D'Agostino-Pearson normality tests. Comparisons were made by paired student t-test and

correlations determined by Spearman's test using Prism 6.0 software (GraphPad Inc.). Significance was defined as $P < 0.05$.

Results

Demographic data for macrophage donors.

The demographic features for the COPD-MAP macrophage donors are listed in Table 1. The COPD patients had a significantly greater number of pack years of cigarette exposure. Sixteen of 42 COPD patients (38.1%) had a history of frequent exacerbations (≥2/year). Vaccine history was available in 69% and of these 83% of COPD patients had received a pneumococcal vaccine.

COPD AM have selective defects in phagocytosis of opsonized S. pneumoniae.

Both COPD AM and MDM demonstrated reduced intracellular numbers of *S. pneumoniae* compared to healthy controls, irrespective of opsonic conditions (Figure 1A-D). COPD AM (but not MDM) from frequent exacerbators had reduced intracellular bacteria, irrespective of opsonic conditions (Figure 1A-D). Frequent exacerbation was set at ≥2 exacerbations/yr. and as shown in Figure E1 patients with only one exacerbation did not have a reduction in bacteria uptake, while those with ≥2 did. Paired analysis of intracellular bacteria numbers, comparing MDM with AM from the same donor, showed that intracellular *S. pneumoniae* were lower in AM than MDM in COPD (but not healthy groups,) regardless of opsonic condition or exacerbation frequency (Figure 1E-F). Opsonization significantly increased numbers of intracellular bacteria in all MDM groups, but significantly increased numbers only in healthy, not COPD, AM (Figure 1G-H).

The number of viable intracellular *S. pneumoniae* is influenced by both phagocytosis and the rate of early intracellular killing (13). To establish that lower intracellular viable bacteria in COPD AM were not due to alterations in bactericidal activity, we measured the kinetics of intracellular killing. Opsonization did not alter the rate of bacterial killing in any macrophages (Figure E2A-D). Opsonization appropriately increased both the percentage of healthy AM binding bacteria, and also the number of internalized bacteria binding per macrophage but did not enhance uptake in COPD (Figure E3). Binding of non-opsonized or opsonized *S. pneumoniae* was not altered by COPD or exacerbation frequency. Surface expression of Fcγ receptors, CD16, CD32 and CD64 were similar in AM/MDM of COPD patients and controls (Figure E4A-B). Studies have demonstrated a central role for the Exchange protein activated by cAMP 1 (Epac-1) in the inhibition of Fc-γ receptor-mediated phagocytosis (20). However, AM expression of Epac-1, or of its primary target Rap-1 (21) was unaltered by *S. pneumoniae* challenge or by COPD (Figure E4C-D). Similarly, there was no difference in expression of Rac1, a Rho-family GTP-binding protein that regulates lamellipodia formation and membrane ruffling in Fc receptor-mediated phagocytosis in AM (22).

Since COPD AM demonstrate a specific defect in opsonic phagocytosis we confirmed if patient bronchoalveolar lavage fluid (BAL) samples had significant levels of anti-pneumococcal antibodies. We measured antibodies against the 13 serotypes included in Prevnar-13, a licensed protein conjugate vaccine, using a sensitive multiplex immunoassay. Unconcentrated BAL samples had detectable pneumococcal antibodies to 2.9 ± 0.5 serotypes and 72% of samples had antibody against at least one serotype, with a range of 0-9 serotypes. Antibodies were most common to serotypes 3 (38%),

serotype 14 (45%) and serotype 19A (45%), see Figure E5. More specifically for the COPD sample 73% had detectable antibodies to 1 or more serotypes.

Decreased opsonic phagocytosis in COPD is associated with bacterial colonisation and correlates with clinical features.

COPD lungs are often colonized with bacteria, most often *H. influenzae* and *S. pneumoniae* (23), and colonization is associated with increased exacerbation frequency (6). Since AM are essential mediators of pulmonary innate immunity (24), we established whether AM phagocytic defects were associated with bacterial colonization. We found that COPD patients who were culture-positive for pathogenic micro-organisms (PPMs) in their sputum had significantly lower levels of AM phagocytosis for opsonized, but not non-opsonized *S. pneumoniae*, when compared to culture-negative patients (Figure 2A-B). In contrast, using qPCR to identify pathogenic micro-organisms in BAL, we determined that PCR-positive samples were not associated with lower levels of opsonic or non-opsonic AM phagocytosis of *S. pneumoniae* (Figure 2C-D).

Correlation analysis of non-opsonized and opsonized phagocytosis of *S. pneumoniae* against FEV_1 showed that there was a significant relationship between FEV_1 and levels of opsonic phagocytosis, but not non-opsonic phagocytosis (Figure 3A-B). However, since FEV_1 correlates poorly with symptoms in COPD (25), we also looked to see if AM phagocytosis levels were related to scores from health-related quality of life (HR-QoL) instruments, the St George's Respiratory Questionnaire (SGRQ), COPD Assessment Test (CAT) or with the 6-minute walking distance (6MW). For the SGRQ and CAT score (although not for the 6MW), there was a significant correlation

between impaired opsonic phagocytosis and scores representative of increased symptom severity but, in contrast, non-opsonic uptake was not correlated with any HR-QoL score, suggesting it was less tightly associated with COPD symptoms (Figure 4A-F).

COPD AM have reduced transcription of antioxidant genes induced in response to opsonized bacteria.

To provide further insights into the mechanisms influencing the selective defect in opsonic phagocytosis in AM we next looked at the transcriptional response of AM to opsonized *S. pneumoniae*. There are significantly fewer differentially expressed genes in the COPD AM in response to infection than in healthy AM (Figure 5A). Table E1-2 shows the top ten upregulated and downregulated gene probes in healthy and COPD AM respectively. We reviewed the enriched GO terms and noted fewer terms differentially regulated in COPD and lower levels of induction (Figure 5B). We also observed that, within the Biological Processes differentially regulated, although the GO term relating to the cellular response to stress was prominently enriched in healthy AM, it comprised significantly fewer components in the COPD AM (supplemental Table E3). Included in this response are a series of genes regulating antioxidant defense, which were prominent in the genes altered in healthy AM (Figure 5C, supplemental Figure E6 and supplemental Table E4), but these showed comparatively less differential regulation in in COPD. Although these responses are not recognized as a major feature of innate host responses to bacteria, antioxidant responses modulate inflammatory responses. These antioxidant responses are activated by a variety of sources of oxidative

stress including microbicidal responses to bacteria and baseline reductions in antioxidant responses are previously described in COPD (26).

Activation of Nrf2 increases phagocytosis of non-opsonized and opsonized S. pneumoniae in AM but not MDM.

Increased oxidative stress in the COPD lung has been associated with impairment of phagocytosis of non-opsonized unencapsulated bacteria and apoptotic bodies (27, 28). The transcription factor Nrf2 is a key regulator of cytoprotective proteins including antioxidants (29, 30) and treatment of macrophages with a pharmacological activator of Nrf2, sulforaphane, increases phagocytosis of non-type able *H. influenzae* (NTHi) and *Pseudomonas aeruginosa* in COPD AM (8). Within the differentially expressed genes in AM following pneumococcal challenge, we identified multiple Nrf2 regulated genes in healthy AM, but these were not differentially regulated in COPD AM (Figure 5C and supplemental Table E5).

Since we identified impairment of an antioxidant transcriptional module we next tested whether sulforaphane modulated phagocytosis of *S. pneumoniae*. We confirmed sulforaphane activated heme-oxygenase (HO-1), an Nrf-2 target gene, in COPD macrophages (Figure 6A-B) and did not induce either apoptosis or necrosis in macrophages (Figure E7). Sulforaphane significantly increased numbers of intracellular bacteria after challenge with non-opsonized *S. pneumoniae* in both healthy and COPD AM (Figure 6C), but after challenge with opsonized *S. pneumoniae* only in COPD (not healthy) AM (Figure 6D). In contrast, we failed to demonstrate an uplift in MDM ingestion under any of the conditions studied (Figure 6E-F). To determine if this pattern occurred with other bacteria, we

confirmed sulforaphane also increased intracellular numbers of NTHi in COPD AM but not healthy AM/MDM or COPD MDM (Figure 6G-H). We also confirmed sulforaphane did not alter the rate of early intracellular killing of *S. pneumoniae* in COPD AM (Figure 6I). Moreover, sulforaphane did not significantly induce expression of Fc-gamma expression (CD16, 32 or 64) in either AM or MDM (Figure E8). To determine if the uplift in phagocytosis was sulforaphane specific, cells were also treated with a more specific Nrf2 agonist, Compound 7. This is a recently described potent and selective inhibitor of the Kelch-like ECH-associated protein 1 (KEAP1) /Nrf-2 protein-protein interaction (16). Treatment with Compound 7, also induced expression of HO-1 in COPD MDM in a concentration-dependent manner (Figure 7A) and importantly glutamate-cysteine ligase catalytic subunit (GCLC) and NADPH:quinone oxidoreductase 1 (NQO1), two of the Nrf2-regulated tragets upregulated by infection,in AM (Figure 7B). Compound 7 significantly increased phagocytosis of opsonized and non-opsonized *S. pneumoniae* by COPD (but not helathy) AM and MDM (Figure 7C-F). As with sulforaphane Compound 7 treatment did not induce cytotoxic effects (Figure E7B). To complete the data set with compound 7 (and for healthy donors in Figure 6G) we added some additional patients recuited outside COPD-MAP, whose demographics are shown in Table E6. These findings illustrate the potential to reverse opsonic phagocytic defects with Nrf2 agonists.

Discussion

We have demonstrated that COPD macrophages have reduced phagocytosis of bacteria. Although we observed defects in MDM phagocytic function, failure to

induce phagocytic uplift by opsonization was unique to COPD AM and was the specific defect that was most predictive of clinical phenotype. COPD AM exposed to opsonized bacteria had decreased transcriptional responses involving antioxidant defenses. Importantly AM defects in bacterial uptake were reversed with Nrf2 agonists.

Several prior publications have demonstrated COPD is associated with impaired macrophage phagocytosis of bacteria and apoptotic cells (8, 9, 10, 31). These studies suggest that there is both a local AM defect but also a systemic defect in macrophage function, which may arise from a combination of genetic, epigenetic and environmental factors. Our study extends our understanding by showing an additional select defect in AM function that inhibits phagocytosis of opsonized bacteria.

Both complement and immunoglobulin are present in alveolar lining fluid (14). Pneumococcal-specific IgG is detected in human BAL (32) and is required for optimal phagocytosis of *S. pneumoniae* by AM (13). Our study also confirms the presence of anti-pneumococcal antibodies in unconcentrated BAL, in a COPD population, in which available data showed >80% vaccination uptake, and an age matched population some of whom would have had vaccine on the basis of age. Therefore, a defect in opsonic uptake could reduce the efficacy of vaccination despite the presence of pneumococcal antibodies in the airway. In a murine model cigarette smoke reduced complement-mediated *S. pneumoniae* uptake, but not phagocytosis of IgG coated beads (33). Impaired phagocytosis of opsonized *S. pneumoniae* and other encapsulated bacteria is likely to contribute to COPD pathogenesis. *S. pneumoniae* remains a leading cause of exacerbations in COPD (5) and in one study monoculture

of *S. pneumoniae* proved a specific risk factor for exacerbation (17). *S. pneumoniae* also have indirect effects on exacerbations since they promote growth, biofilm formation and synergy in inflammatory responses with other bacteria causing exacerbations (34-36). In addition, *S. pneumoniae* is the major cause of CAP in these patients (37), and COPD increases the susceptibility and risk of complications with CAP (7).

Recent observations involving polymeric immunoglobulin receptor deficient mice illustrate how bacterial persistence drives inflammation and small airway remodelling in a model of COPD (38). Bacterial colonization of the airways is linked to decline in lung function (6, 39) and recently, bacterial phagocytosis has been shown to correlate with FEV_1 in both COPD (40) and severe asthma (41). Reduced phagocytosis of opsonized bacteria by AM was observed in patients who were culture-positive, although PCR-positivity in BAL was not associated with the level of phagocytosis. It would be of interest in the future to determine if opsonic phagocytosis correlates with quantitation of PCR but our numbers did not allow this analysis. We used a threshold of $>10^4$ copies/ml to define positivity. Although this threshold ensures sensitivity and a high negative predictive value in studies on the detection of lower respiratory tract infection due to organisms such as *S. pneumoniae* and *H. influenzae* (42, 43) it may under estimate colonization. On the other hand, the detection of colonization by PCR with lower level PCR thresholds is problematic and diagnostic accuracy may be influenced by increasing numbers of false positive results. Therefore, the sputum detection may have been more predictive of colonization status. The defect in AM phagocytosis of opsonized bacteria was more severe in COPD patients with frequent exacerbations, a factor associated with more rapid decline in FEV_1 (44). This could

explain the correlations we observed with more significant impairment of opsonic phagocytosis observed in patients with lower FEV_1 or more severe symptoms with quality of life assessments. Assessment scales are widely used to describe COPD patient cohorts and stratify them for interventions, such as pulmonary rehabilitation (45) and to predict survival (46). Quality of life scales are complementary to FEV_1 in describing disability (e.g. MRC dyspnea scale) or severity of dyspnea symptoms (e.g. COPD assessment test) in patients living with COPD and it was noteworthy that the SGRQ and CAT correlated with the defect for phagocytosis of opsonized bacteria. FEV_1 provides a measure of COPD stage, but correlates poorly with symptoms (25). This implies the phagocytic defect may be related both to stage and symptoms.

Future studies will need to identify if the phagocytic defect for opsonized bacteria is related to a specific receptor pathway or cytoskeletal re-arrangement. A prior study identified a defect in macrophage receptor with collagenous structure (MARCO) mediated phagocytosis in COPD (8). This important study identified impaired phagocytosis of two non-opsonized bacteria (NTHi and *P. aeruginosa*) in COPD AM and mice exposed to cigarette smoke and showed that sulforaphane corrected the defect in an Nrf2-dependent mechanism via enhanced MARCO expression. Our study in a population with very few current smokers is consistent with these findings confirming a defect in phagocytosis of non-opsonized bacteria (*S. pneumoniae* and NTHi), which is improved by Nrf2 agonists. We extend beyond this showing an additional defect for opsonized *S. pneumoniae.* In contrast to the study by Harvey and colleagues our study highlighted transcriptional changes associated with infection in healthy and COPD AM rather than the transcriptional effects of sulforaphane, but also highlights reductions in Nrf2-mediated responses in COPD AM. The range of

particles, including both opsonized and non-opsonized bacteria and apoptotic bodies, for which defects have been identified in COPD, argues against involvement of any single receptor system underlying all these defects. Although MARCO likely contributes to defects in uptake of non-opsonized bacteria (8), it would not be anticipated to explain the impairment of opsonized bacteria by AM. An unbiased approach is more likely to identify mechanisms underpinning the broad systemic defect in phagocytosis and the more localized pulmonary defect for opsonized bacteria.

The transcriptional responses seen in the healthy AM, in response to *S. pneumoniae* included prominent transcriptional responses involving immunometabolism. The acute responses to bacteria results in a shift to increased glucose uptake and glycolytic metabolism (47), while glucose diversion via the pentose phosphate pathway is a well-recognized mechanism of oxidative stress resistance (48). Amongst differentially expressed metabolic genes increased in healthy but not COPD AM was sirtuin (silent mating type information regulation 2 homologs) 1, a deacetylase involved in host responses to *M. tuberculosis* (49). Anti-oxidant responses were prominently upregulated in healthy AM after bacterial infection. Nrf2 regulated genes included GCLC, glutathione-S-transferase zeta 1 (GSTZ-1), glutathione peroxidase 7 (GPX7) and the SLC7A11 gene product, light chain subunit of the Xc^- (xCT) glutamine/cysteine antiporter required, all involved in glutathione maintenance and utilization, carbonyl reductase 1 (CBR1), NQO1, and thioredoxin 2 (TXN2) detoxifying oxidoreductase enzymes and superoxide dismutase (SOD) 1 (48). Foxo-regulated targets including SOD 2 were upregulated, while p53 was also upregulated. Of all these anti-oxidant responses only p53 was significantly upregulated in COPD

AM after bacterial challenge. We identified upregulation of a series of genes involved in regulation of ubiquitination (including ubiquitin conjugating E2 enzymes B, D3 and N), a process controlling signaling via pattern recognition receptors, in healthy AM after bacterial challenge (50). Collectively these anti-oxidant responses have the potential to alter cytokine-induced activation of specific phagocytic pathways, expression of receptors or molecules involved in signaling cascades associated with receptors or the susceptibility of the cytoskeleton to re-arrangements altered by oxidative stress required for particular phagocytic pathways. It was noteworthy that the transcriptional response in healthy AM involved downregulation of the class B scavenger receptor CD36, a receptor for unopsonized particles (51) , which was not observed in COPD AM.

The Nrf2 transcription factor regulates a cluster of antioxidant, cytoprotective and detoxifying genes and influences susceptibility to COPD in murine models involving cigarette smoke exposure by modifying inflammation and tissue injury (52). We confirmed prior observations suggesting Nrf2 agonists correct the phagocytic defect in COPD (8), but extend these by showing they also modulate phagocytosis of opsonized bacteria. Since this also influenced uptake of non-opsonized particles it is likely Nrf2 agonists have pleiotropic effects in the modulation of phagocytosis. Nrf2 agonists represent a promising class of agents with which to modulate oxidative stress in conditions like COPD, particularly with the development of highly-selective agents that bind to the Kelch domain of KEAP1 and prevent Nrf2 ubiquitination and proteasomal degradation (16). While sulforaphane activates Nrf2 by targeting cysteine residues in the BTB domain of KEAP1 and can potentially interact with other targets (53) we demonstrate significant enhancement of phagocytosis in COPD

macrophages with the selective Nrf2 agonist Compound 7, suggesting this could represent a potent pharmacological approach with which to correct the COPD associated defects in phagocytosis.

In conclusion we have identified that, although COPD induces a systemic defect in a range of forms of phagocytosis, a specific defect in phagocytosis of opsonized bacteria is observed specifically in AM and correlates closely with clinical phenotype in COPD. Moreover, this defect is amenable to therapeutic targeting with novel and selective inhibitors of the KEAP1/Nrf2 protein-protein interaction.

Acknowledgements.

We would like to thank Prof. Ian Sabroe in setting up ethics approvals for research bronchoscopies and in for discussions on pulmonary host defense. This report is independent research supported by National Institute for Health Research (NIHR) South Manchester Respiratory and Allergy Clinical Research Facility at University Hospital of South Manchester NHS Foundation Trust and the NIHR Clinical Research Facility at Sheffield Teaching Hospitals Foundation Trust. The views expressed in this publication are those of the author(s) and not necessarily those of the NHS, the National Institute for Health Research or the Department of Health.

Figure Legends

Figure 1. COPD AM show deficient opsonic bacterial phagocytosis which correlates with exacerbation frequency. (A-D) Alveolar macrophages (AM) (A and B) or monocyte-derived macrophages (MDM) (C and D) from healthy (H) or COPD (non-frequent (NF) and frequent (F) exacerbators) were challenged with either non-opsonized (A and C) or opsonized (B and D) serotype 14 *S. pneumoniae.* 4h post-challenge *viable* intracellular bacteria were assessed. Values for 'n=' for H/COPD-NF/COPD-F; (A) 18/27/15, (B) 10/19/13, (C) 14/18/12, (D) 14/15/12, ***= $p<0.001$, 1-way ANOVA. **(E-F)** A pairwise comparison of phagocytosis of non-opsonized (E) and opsonized (F) bacteria in MDM and AM from matched donors, ns= not significant, values for 'n=' for H/COPD-NF/COPD-F; (E) 11/12/12, (F) 10/11/12, *=$p<0.05$, **=$p<0.01$, ***=$p<0.001$, paired t-test. (**G-H)** A pairwise comparison of phagocytosis of non-opsonized and opsonized *S. pneumoniae* in matched AM (G) or MDM (H) donors, values for 'n=' for H/COPD-NF/COPD-F; (G) 10/20/11, (H) 7/8/5, *=$p<0.05$, paired t-test.

Figure 2. Defects in phagocytosis in COPD AM are associated with bacterial colonisation in the lung. (A-D) Non-opsonic (A and C) and opsonic (B and D) phagocytosis was stratified into groups dependent on if the donor had negative (-ve) or positive (+ve) culture of sputum (A and B, n=15 and n=14) or –ve or +ve (defined as $>10^4$ copies/ml) qPCR of broncho-alveolar lavage (C and D, n=27 and n=26) results indicative of bacterial colonisation, *=$p<0.05$, Student's t-test.

Figure 3. Opsonic phagocytosis correlates with FEV_1. Non-opsonic (A) and opsonic (B) phagocytosis rates were correlated against patient FEV_1 score. Pearson's correlation coefficients (r), and p values, with correlation deemed significant if $p<0.05$. n = 36 non-opsonic, 32 opsonic.

Figure 4. Opsonic phagocytosis correlates with markers of COPD disease severity. Non-opsonic (A, C and E) and opsonic (B, D and F) rates of phagocytosis were correlated against patients scores in a variety of markers for COPD disease severity, the St George's Respiratory Questionnaire (SGRQ) (A and B) (n = 29 non-opsonic, 27 opsonic), COPD Assessment Test (CAT) (C and D) (n = 34 non-opsonic, 30 opsonic) or with the 6-minute walking distance (6MW) (E and F) (n = 14 non-opsonic, 10 opsonic). Values for Pearson's (r) or Spearman's correlation coefficients (rho) and p values are shown, with correlation deemed significant if p= <0.05.

Figure 5. Transcriptional response of AM reveals less differential gene expression in COPD in response to infection. Alveolar macrophages (AM) from Healthy or COPD patients were challenged with opsonized serotype 14 *S. pneumoniae* (n=3 in each group). 4h post-challenge cell total RNA was collected for transcriptional analysis. **(A)** Venn diagram showing the number of probes differentially expressed in response to infection (moderated t test <0.05, FDR <0.05). **(B)** Plots represent the top ten enriched GO biological processes terms and the cellular response to stress term (in addition the response to oxidative stress term is plotted in the Healthy AM). The X axis represents enrichment by a hypergeometric test (–log10 (p value)). The size of the circle and colour represents the number of differentially expressed genes in that term. Figures generated using NIPA (available

at https://github.com/ADAC-UoN/NIPA). **(C)** Volcano plots represent the probe sets identified from the transcriptomic analysis. Panel a) Healthy: The red triangles are the differentially expressed probes related to the "Cellular response to stress term" with some representative terms named. In blue are the terms associated with the Nrf-2 pathway in the analysis of healthy AM. Panel b) COPD: The red triangles are the differentially expressed probes related to the "Cellular response to stress" GO term. In blue are the terms associated with NRF2 pathway seen in the Healthy analysis.

Figure 6. Treatment with the Nrf-2 agonist sulforaphane increases non-opsonic and opsonic phagocytosis in COPD AM but not MDM. (A-B) Alveolar macrophages (AM) and monocyte derived macrophages (MDM)(B) were pre-treated with the designated dose of sulforaphane (Sulf) for 16h, before cells were lysed and probed for expression of heme-oxygenase-1 (HO-1) and actin (n=3). **(C-F)** AM (C-D) or MDM (E and F) from healthy (H) or COPD non-frequent (NF) or frequent (F) exacerbators were pre-treated with vehicle (Sulf -) or Sulforaphane (Sulf +) for 16 h, before cells were challenged with non-opsonized (C and E) or opsonized (D and F) serotype 14 *S. pneumoniae*. 4h post-challenge, numbers of intracellular viable bacteria were measured, values for 'n=' for H/COPD-NF/COPD-F; (C) 11/19/14, (D) 8/ 10/4, (E) 9/9/5, (F) 8/9/5, *=$p<0.05$, paired t-test. **(G and H)** AM (G) and MDM (H) from COPD patients or healthy (H) donors were pre-treated with sulforaphane before being challenged with non-typeable *H. influenzae* (NTHi). 4h post challenge the numbers of intracellular viable bacteria were measured, values for 'n=' for H/COPD (G)3/4, (H) 3/3, *=$p<0.05$, paired t-test. **(I)** COPD AM were pre-treated with sulforaphane (+Sulf) before being challenged with non-opsonized serotype 14 *S. pneumoniae* for 4h before extracellular bacteria were killed by the addition of antibiotics. At the designated time

post-antibiotics, viable bacteria in duplicate wells were measured to, n=3, no significant difference between vehicle and sulf.

Figure 7. The Nrf-2 agonist compound 7 also increases phagocytosis in COPD AM.

(A and B) COPD monocyte-derived macrophages (MDM) (A), or alveolar macrophages (AM) (B), were pre-treated with the Nrf-2 agonist Compound 7 for 16h at the designated dose, before cells were lysed and a probed for the expression of heme-oxygenase-1 (HO-1), glutamate-cysteine ligase catalytic subunit (GCLC) or NADPH:quinone oxidoreductase 1 (NQO1) by western blot. **(C and D)** Healthy donor and COPD AM were pre-treated with Compound 7 at 5x IC_{50} (0.065 μM), for 16h before being challenged with opsonized (C), n=3 healthy, n=5 COPD or non-opsonized (D), n=3 healthy, n=10 COPD, serotype 14 *S. pneumoniae* for 4h, after which numbers of intracellular viable bacteria were assessed, **=$p<0.01$, paired t-test. **(E and F)** Healthy donor and COPD MDM were pre-treated with compound 7 and challenged with opsonized (E), or non-opsonized (F), *S. pneumoniae* as for AM. All n=4, p **=$p<0.01$, paired t-test.

References

1. Vogelmeier CF, Criner GJ, Martinez FJ, Anzueto A, Barnes PJ, Bourbeau J, Celli BR, Chen R, Decramer M, Fabbri LM, Frith P, Halpin DM, Lopez Varela MV, Nishimura M, Roche N, Rodriguez-Roisin R, Sin DD, Singh D, Stockley R, Vestbo J, Wedzicha JA, Agusti A. Global strategy for the diagnosis, management, and prevention of chronic obstructive lung disease 2017 report. Gold executive summary. *Am J Respir Crit Care Med* 2017;195:557-582.
2. Barnes PJ. Alveolar macrophages in chronic obstructive pulmonary disease (copd). *Cellular and molecular biology* 2004;50 Online Pub:OL627-637.
3. Hurst JR, Vestbo J, Anzueto A, Locantore N, Mullerova H, Tal-Singer R, Miller B, Lomas DA, Agusti A, Macnee W, Calverley P, Rennard S, Wouters EF, Wedzicha JA. Susceptibility to exacerbation in chronic obstructive pulmonary disease. *The New England journal of medicine* 2010;363:1128-1138.
4. Seemungal TA, Donaldson GC, Paul EA, Bestall JC, Jeffries DJ, Wedzicha JA. Effect of exacerbation on quality of life in patients with chronic obstructive pulmonary disease. *Am J Respir Crit Care Med* 1998;157:1418-1422.
5. Sapey E, Stockley RA. Copd exacerbations . 2: Aetiology. *Thorax* 2006;61:250-258.
6. Patel IS, Seemungal TA, Wilks M, Lloyd-Owen SJ, Donaldson GC, Wedzicha JA. Relationship between bacterial colonisation and the frequency, character, and severity of copd exacerbations. *Thorax* 2002;57:759-764.
7. Restrepo MI, Mortensen EM, Pugh JA, Anzueto A. Copd is associated with increased mortality in patients with community-acquired pneumonia. *Eur Respir J* 2006;28:346-351.
8. Harvey CJ, Thimmulappa RK, Sethi S, Kong X, Yarmus L, Brown RH, Feller-Kopman D, Wise R, Biswal S. Targeting nrf2 signaling improves bacterial clearance by alveolar macrophages in patients with copd and in a mouse model. *Science translational medicine* 2011;3:78ra32.
9. Berenson CS, Wrona CT, Grove LJ, Maloney J, Garlipp MA, Wallace PK, Stewart CC, Sethi S. Impaired alveolar macrophage response to haemophilus antigens in chronic obstructive lung disease. *Am J Respir Crit Care Med* 2006;174:31-40.
10. Taylor AE, Finney-Hayward TK, Quint JK, Thomas CM, Tudhope SJ, Wedzicha JA, Barnes PJ, Donnelly LE. Defective macrophage phagocytosis of bacteria in copd. *Eur Respir J* 2010;35:1039-1047.
11. Palecanda A, Kobzik L. Receptors for unopsonized particles: The role of alveolar macrophage scavenger receptors. *Current molecular medicine* 2001;1:589-595.
12. Aderem A, Underhill DM. Mechanisms of phagocytosis in macrophages. *Annual review of immunology* 1999;17:593-623.
13. Gordon SB, Irving GR, Lawson RA, Lee ME, Read RC. Intracellular trafficking and killing of streptococcus pneumoniae by human alveolar macrophages are influenced by opsonins. *Infection and immunity* 2000;68:2286-2293.
14. Nicod LP. Lung defences: An overview. *European Respiratory Review* 2005;14:45-50.
15. Bewley MA. Copd alveolar macrophages have a defect in opsonic phagocytosis of serotype 14 streptococcus pneumoniae. . 2014;189.
16. Davies TG, Wixted WE, Coyle JE, Griffiths-Jones C, Hearn K, McMenamin R, Norton D, Rich SJ, Richardson C, Saxty G, Willems HM, Woolford AJ, Cottom JE, Kou JP, Yonchuk JG, Feldser HG, Sanchez Y, Foley JP, Bolognese BJ, Logan G,

Podolin PL, Yan H, Callahan JF, Heightman TD, Kerns JK. Monoacidic inhibitors of the kelch-like ech-associated protein 1: Nuclear factor erythroid 2-related factor 2 (keap1:Nrf2) protein-protein interaction with high cell potency identified by fragment-based discovery. *Journal of medicinal chemistry* 2016;59:3991-4006.
17. Bogaert D, van der Valk P, Ramdin R, Sluijter M, Monninkhof E, Hendrix R, de Groot R, Hermans PW. Host-pathogen interaction during pneumococcal infection in patients with chronic obstructive pulmonary disease. *Infect Immun* 2004;72:818-823.
18. Dockrell DH, Lee M, Lynch DH, Read RC. Immune-mediated phagocytosis and killing of streptococcus pneumoniae are associated with direct and bystander macrophage apoptosis. *The Journal of infectious diseases* 2001;184:713-722.
19. Marriott HM, Ali F, Read RC, Mitchell TJ, Whyte MK, Dockrell DH. Nitric oxide levels regulate macrophage commitment to apoptosis or necrosis during pneumococcal infection. *FASEB journal : official publication of the Federation of American Societies for Experimental Biology* 2004;18:1126-1128.
20. Aronoff DM, Canetti C, Serezani CH, Luo M, Peters-Golden M. Cutting edge: Macrophage inhibition by cyclic amp (camp): Differential roles of protein kinase a and exchange protein directly activated by camp-1. *Journal of immunology* 2005;174:595-599.
21. de Rooij J, Zwartkruis FJ, Verheijen MH, Cool RH, Nijman SM, Wittinghofer A, Bos JL. Epac is a rap1 guanine-nucleotide-exchange factor directly activated by cyclic amp. *Nature* 1998;396:474-477.
22. Castellano F, Montcourrier P, Chavrier P. Membrane recruitment of rac1 triggers phagocytosis. *Journal of cell science* 2000;113 (Pt 17):2955-2961.
23. Wedzicha JA, Donaldson GC. Exacerbations of chronic obstructive pulmonary disease. *Respir Care* 2003;48:1204-1213; discussion 1213-1205.
24. Dockrell DH, Whyte MK, Mitchell TJ. Pneumococcal pneumonia: Mechanisms of infection and resolution. *Chest* 2012;142:482-491.
25. Agusti A, Calverley PM, Celli B, Coxson HO, Edwards LD, Lomas DA, MacNee W, Miller BE, Rennard S, Silverman EK, Tal-Singer R, Wouters E, Yates JC, Vestbo J. Characterisation of copd heterogeneity in the eclipse cohort. *Respiratory research* 2010;11:122.
26. Tuder RM, Petrache I. Pathogenesis of chronic obstructive pulmonary disease. *J Clin Invest* 2012;122:2749-2755.
27. Marti-Lliteras P, Regueiro V, Morey P, Hood DW, Saus C, Sauleda J, Agusti AG, Bengoechea JA, Garmendia J. Nontypeable haemophilus influenzae clearance by alveolar macrophages is impaired by exposure to cigarette smoke. *Infection and immunity* 2009;77:4232-4242.
28. Richens TR, Linderman DJ, Horstmann SA, Lambert C, Xiao YQ, Keith RL, Boe DM, Morimoto K, Bowler RP, Day BJ, Janssen WJ, Henson PM, Vandivier RW. Cigarette smoke impairs clearance of apoptotic cells through oxidant-dependent activation of rhoa. *Am J Respir Crit Care Med* 2009;179:1011-1021.
29. Goven D, Boutten A, Lecon-Malas V, Marchal-Somme J, Amara N, Crestani B, Fournier M, Leseche G, Soler P, Boczkowski J, Bonay M. Altered nrf2/keap1-bach1 equilibrium in pulmonary emphysema. *Thorax* 2008;63:916-924.
30. Zhao H, Eguchi S, Alam A, Ma D. The role of nuclear factor-erythroid 2 related factor 2 (nrf-2) in the protection against lung injury. *American journal of physiology Lung cellular and molecular physiology* 2017;312:L155-L162.
31. Hodge S, Hodge G, Scicchitano R, Reynolds PN, Holmes M. Alveolar macrophages from subjects with chronic obstructive pulmonary disease are deficient

in their ability to phagocytose apoptotic airway epithelial cells. *Immunol Cell Biol* 2003;81:289-296.
32. Eagan R, Twigg HL, 3rd, French N, Musaya J, Day RB, Zijlstra EE, Tolmie H, Wyler D, Molyneux ME, Gordon SB. Lung fluid immunoglobulin from hiv-infected subjects has impaired opsonic function against pneumococci. *Clin Infect Dis* 2007;44:1632-1638.
33. Phipps JC, Aronoff DM, Curtis JL, Goel D, O'Brien E, Mancuso P. Cigarette smoke exposure impairs pulmonary bacterial clearance and alveolar macrophage complement-mediated phagocytosis of streptococcus pneumoniae. *Infection and immunity* 2010;78:1214-1220.
34. Bosch AA, Biesbroek G, Trzcinski K, Sanders EA, Bogaert D. Viral and bacterial interactions in the upper respiratory tract. *PLoS Pathog* 2013;9:e1003057.
35. Ratner AJ, Aguilar JL, Shchepetov M, Lysenko ES, Weiser JN. Nod1 mediates cytoplasmic sensing of combinations of extracellular bacteria. *Cell Microbiol* 2007;9:1343-1351.
36. Tikhomirova A, Kidd SP. Haemophilus influenzae and streptococcus pneumoniae: Living together in a biofilm. *Pathog Dis* 2013;69:114-126.
37. Torres A, Dorca J, Zalacain R, Bello S, El-Ebiary M, Molinos L, Arevalo M, Blanquer J, Celis R, Iriberri M, Prats E, Fernandez R, Irigaray R, Serra J. Community-acquired pneumonia in chronic obstructive pulmonary disease: A spanish multicenter study. *Am J Respir Crit Care Med* 1996;154:1456-1461.
38. Richmond BW, Brucker RM, Han W, Du RH, Zhang Y, Cheng DS, Gleaves L, Abdolrasulnia R, Polosukhina D, Clark PE, Bordenstein SR, Blackwell TS, Polosukhin VV. Airway bacteria drive a progressive copd-like phenotype in mice with polymeric immunoglobulin receptor deficiency. *Nat Commun* 2016;7:11240.
39. Hill AT, Campbell EJ, Hill SL, Bayley DL, Stockley RA. Association between airway bacterial load and markers of airway inflammation in patients with stable chronic bronchitis. *The American journal of medicine* 2000;109:288-295.
40. Berenson CS, Kruzel RL, Eberhardt E, Sethi S. Phagocytic dysfunction of human alveolar macrophages and severity of chronic obstructive pulmonary disease. *The Journal of infectious diseases* 2013;208:2036-2045.
41. Liang Z, Zhang Q, Thomas CM, Chana KK, Gibeon D, Barnes PJ, Chung KF, Bhavsar PK, Donnelly LE. Impaired macrophage phagocytosis of bacteria in severe asthma. *Respiratory research* 2014;15:72.
42. Blaschke AJ. Interpreting assays for the detection of streptococcus pneumoniae. *Clin Infect Dis* 2011;52 Suppl 4:S331-337.
43. Abdeldaim GM, Stralin K, Korsgaard J, Blomberg J, Welinder-Olsson C, Herrmann B. Multiplex quantitative pcr for detection of lower respiratory tract infection and meningitis caused by streptococcus pneumoniae, haemophilus influenzae and neisseria meningitidis. *BMC Microbiol* 2010;10:310.
44. Donaldson GC, Seemungal TA, Bhowmik A, Wedzicha JA. Relationship between exacerbation frequency and lung function decline in chronic obstructive pulmonary disease. *Thorax* 2002;57:847-852.
45. Wedzicha JA, Bestall JC, Garrod R, Garnham R, Paul EA, Jones PW. Randomized controlled trial of pulmonary rehabilitation in severe chronic obstructive pulmonary disease patients, stratified with the mrc dyspnoea scale. *Eur Respir J* 1998;12:363-369.
46. Nishimura K, Izumi T, Tsukino M, Oga T. Dyspnea is a better predictor of 5-year survival than airway obstruction in patients with copd. *Chest* 2002;121:1434-1440.

47. Tannahill GM, Curtis AM, Adamik J, Palsson-McDermott EM, McGettrick AF, Goel G, Frezza C, Bernard NJ, Kelly B, Foley NH, Zheng L, Gardet A, Tong Z, Jany SS, Corr SC, Haneklaus M, Caffrey BE, Pierce K, Walmsley S, Beasley FC, Cummins E, Nizet V, Whyte M, Taylor CT, Lin H, Masters SL, Gottlieb E, Kelly VP, Clish C, Auron PE, Xavier RJ, O'Neill LA. Succinate is an inflammatory signal that induces il-1beta through hif-1alpha. *Nature* 2013;496:238-242.
48. Gorrini C, Harris IS, Mak TW. Modulation of oxidative stress as an anticancer strategy. *Nat Rev Drug Discov* 2013;12:931-947.
49. Cheng CY, Gutierrez NM, Marzuki MB, Lu X, Foreman TW, Paleja B, Lee B, Balachander A, Chen J, Tsenova L, Kurepina N, Teng KWW, West K, Mehra S, Zolezzi F, Poidinger M, Kreiswirth B, Kaushal D, Kornfeld H, Newell EW, Singhal A. Host sirtuin 1 regulates mycobacterial immunopathogenesis and represents a therapeutic target against tuberculosis. *Sci Immunol* 2017;2.
50. Zinngrebe J, Montinaro A, Peltzer N, Walczak H. Ubiquitin in the immune system. *EMBO Rep* 2014;15:28-45.
51. Febbraio M, Hajjar DP, Silverstein RL. Cd36: A class b scavenger receptor involved in angiogenesis, atherosclerosis, inflammation, and lipid metabolism. *J Clin Invest* 2001;108:785-791.
52. Rangasamy T, Cho CY, Thimmulappa RK, Zhen L, Srisuma SS, Kensler TW, Yamamoto M, Petrache I, Tuder RM, Biswal S. Genetic ablation of nrf2 enhances susceptibility to cigarette smoke-induced emphysema in mice. *J Clin Invest* 2004;114:1248-1259.
53. Hu C, Eggler AL, Mesecar AD, van Breemen RB. Modification of keap1 cysteine residues by sulforaphane. *Chem Res Toxicol* 2011;24:515-521.

Table 1: Demographics of Macrophage Donors

	Healthy Non-Smoker	Healthy Ex-Smoker	COPD
N	12	6	42
Age (years)	56 (43-65)	58 (48-69)	66(53-77)
Gender	6♀ : 6♂	2♀ : 4♂	7♀ : 35♂
FEV1 Litres	3.19 (2.25-4.77)	2.99 (2.50-3.70)	1.88 (1.00-2.72)
FEV1 %	110 (74-127)	108 (84-121)	50.8 (32-67)
FVC litres	3.76 (2.25-5.6)	4.19 (3.45-5.2)	3.49 (1.86-5.24)
GOLD Stage *	N/A	N/A	9 GOLD A 14 GOLD B 4 GOLD C 10 GOLD D
Non-Frequent /Frequent**	N/A	N/A	NF 26 (0 Exacerbations = 19, 1 Exacerbation = 7 F 16 (2 Exacerbations =3, 3 Exacerbations =7, >3 Exacerbations =6)
Pack Years	N/A	18 (10-35)	50 (32-67)
Smoking Status: Current/Ex/Never	0/0/12	0/6/0	7/35/0
Inhaled Corticosteroids use	0	0	35
Vaccine	N/A	N/A	24 Yes, 5 No, 13N/A
St George's Respiratory Questionnaire (SGRQ) Total score	N/A	N/A	39.8 (6-83)
COPD Assessment Test (CAT)	N/A	N/A	16.3 (4-33)
6 Minute Walk (m)	N/A	N/A	400 (264-496)

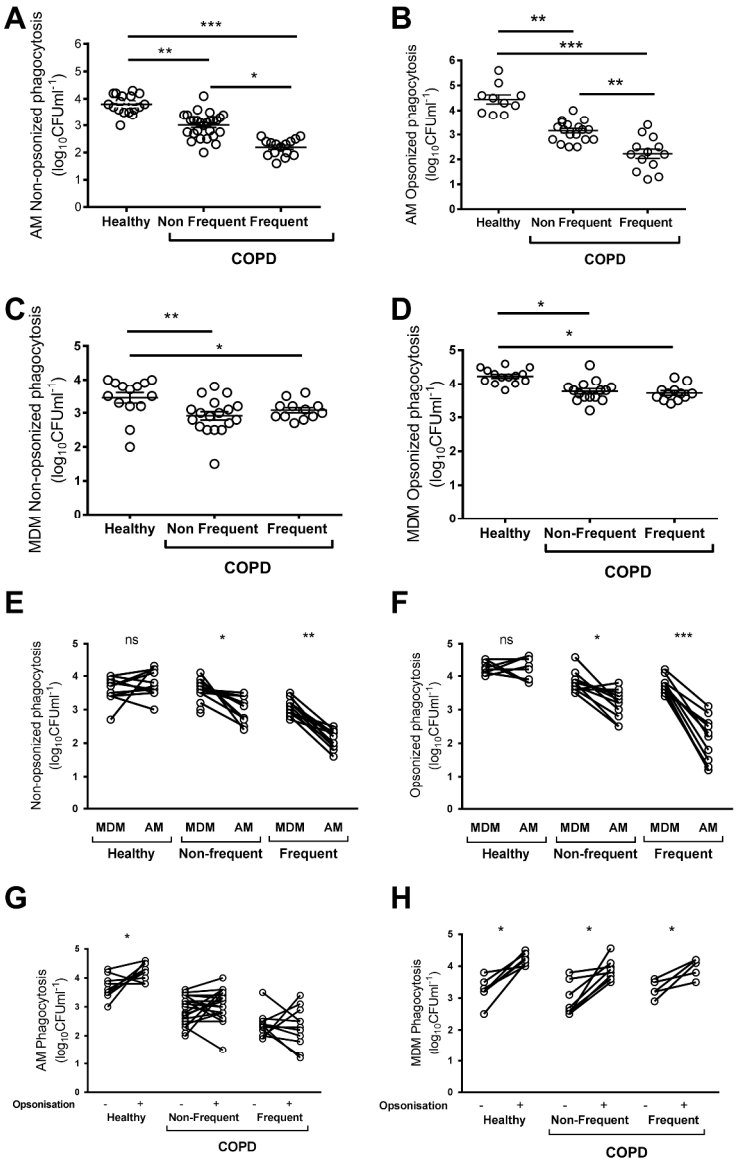

Figure 1. COPD AM show deficient opsonic bacterial phagocytosis which correlates with exacerbation frequency. (A-D) Alveolar macrophages (AM) (A and B) or monocyte-derived macrophages (MDM) (C and D) from healthy (H) or COPD (non-frequent (NF) and frequent (F) exacerbators) were challenged with either non-opsonized (A and C) or opsonized (B and D) serotype 14 S. pneumoniae. 4h post-challenge viable intracellular bacteria were assessed. Values for 'n=' for H/COPD-NF/COPD-F; (A) 18/27/15, (B) 10/19/13, (C) 14/18/12, (D) 14/15/12, ***= p<0.001, 1-way ANOVA. (E-F) A pairwise comparison of phagocytosis of non-opsonized (E) and opsonized (F) bacteria in MDM and AM from matched donors, ns= not significant, values for 'n=' for H/COPD-NF/COPD-F; (E) 11/12/12, (F) 10/11/12, *=p<0.05, **=p<0.01, ***=p<0.001, paired t-test. (G-H) A pairwise comparison of phagocytosis of non-opsonized and opsonized S. pneumoniae in matched AM (G) or MDM (H) donors, values for 'n=' for H/COPD-NF/COPD-F; (G) 10/20/11, (H) 7/8/5, *=p<0.05, paired t-test.

277x418mm (300 x 300 DPI)

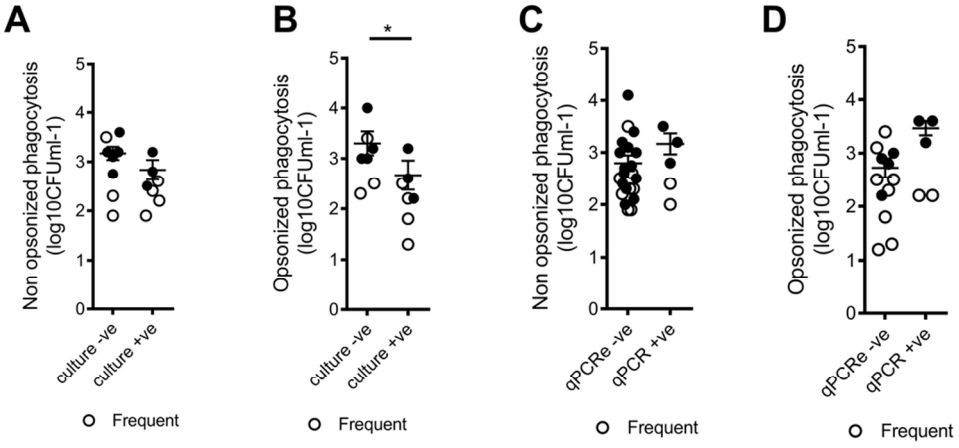

Figure 2. Defects in phagocytosis in COPD AM are associated with bacterial colonisation in the lung. (A-D) Non-opsonic (A and C) and opsonic (B and D) phagocytosis was stratified into groups dependent on if the donor had negative (-ve) or positive (+ve) culture of sputum (A and B, n=15 and n=14) or -ve or +ve (defined as >104 copies/ml) qPCR of broncho-alveolar lavage (C and D, n=27 and n=26) results indicative of bacterial colonisation, *=p<0.05, Student's t-test.

96x47mm (300 x 300 DPI)

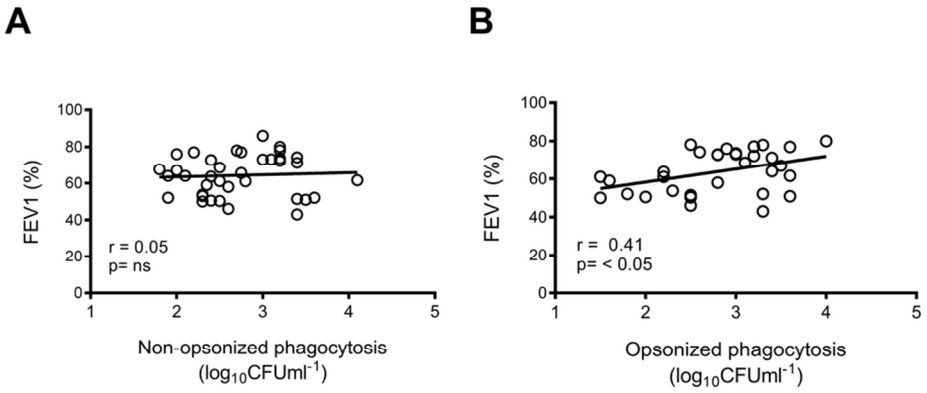

Figure 3. Opsonic phagocytosis correlates with FEV1. Non-opsonic (A) and opsonic (B) phagocytosis rates were correlated against patient FEV1 score. Pearson's correlation coefficients (r), and p values, with correlation deemed significant if $p<0.05$. n = 36 non-opsonic, 32 opsonic.

89x41mm (300 x 300 DPI)

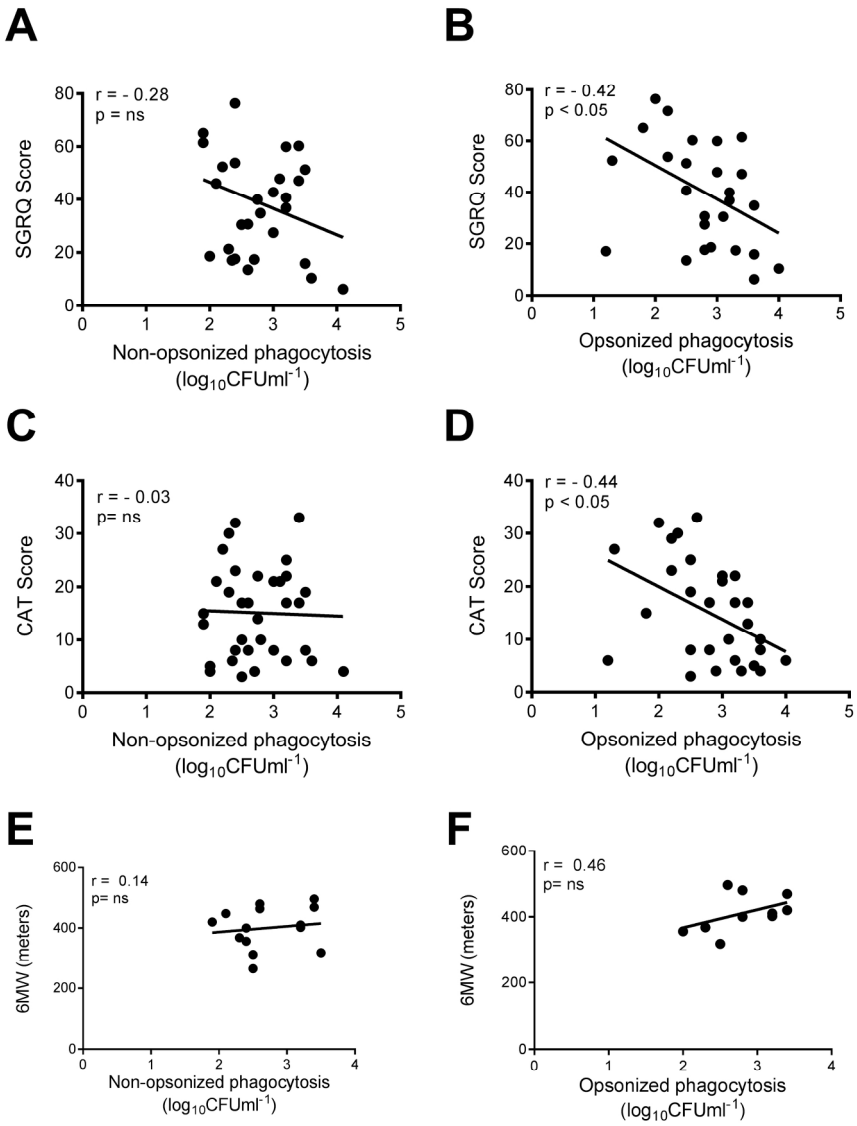

Figure 4. Opsonic phagocytosis correlates with markers of COPD disease severity. Non-opsonic (A, C and E) and opsonic (B, D and F) rates of phagocytosis were correlated against patients scores in a variety of markers for COPD disease severity, the St George's Respiratory Questionnaire (SGRQ) (A and B) (n = 29 non-opsonic, 27 opsonic), COPD Assessment Test (CAT) (C and D) (n = 34 non-opsonic, 30 opsonic) or with the 6-minute walking distance (6MW) (E and F) (n = 14 non-opsonic, 10 opsonic). Values for Pearson's (r) or Spearman's correlation coefficients (rho) and p values are shown, with correlation deemed significant if p= <0.05.

188x237mm (300 x 300 DPI)

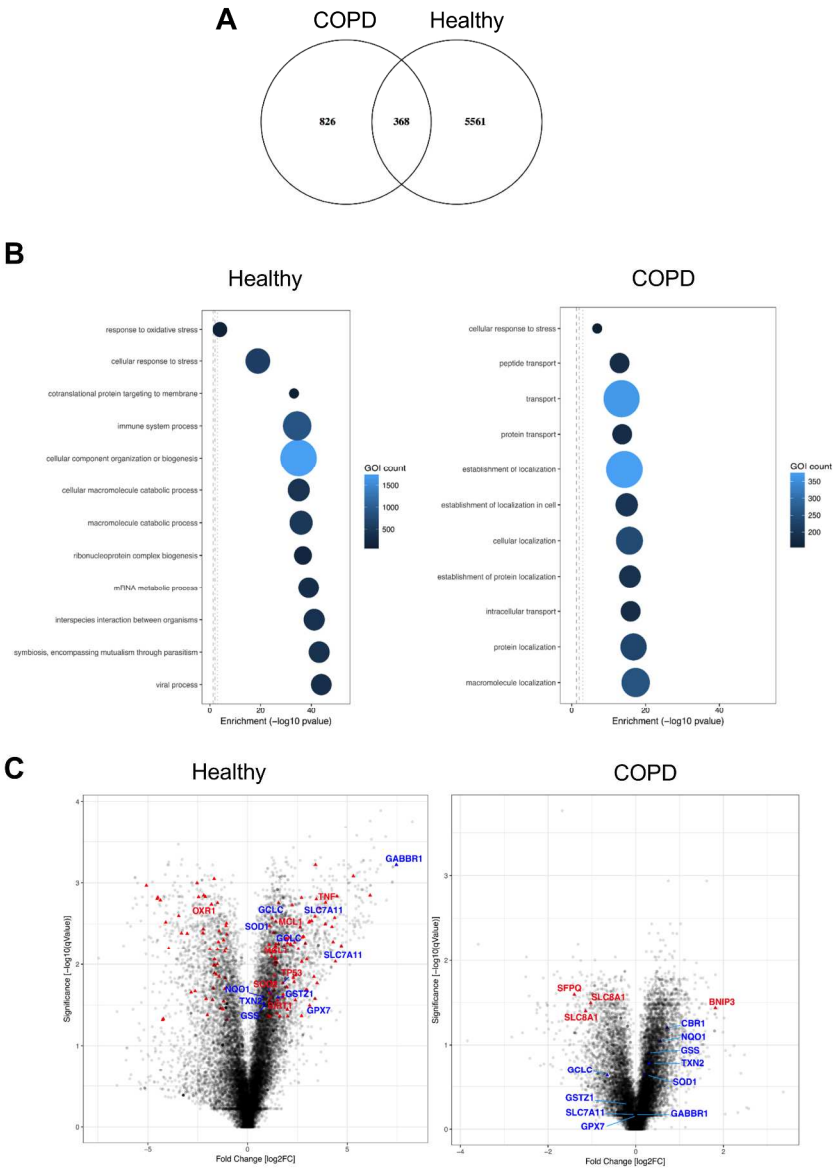

Figure 5. Transcriptional response of AM reveals less differential gene expression in COPD in response to infection. Alveolar macrophages (AM) from Healthy or COPD patients were challenged with opsonized serotype 14 S. pneumoniae (n=3 in each group). 4h post-challenge cell total RNA was collected for transcriptional analysis. (A) Venn diagram showing the number of probes differentially expressed in response to infection (moderated t test <0.05, FDR <0.05). (B) Plots represent the top ten enriched GO biological processes terms and the cellular response to stress term (in addition the response to oxidative stress term is plotted in the Healthy AM). The X axis represents enrichment by a hypergeometric test (-log10 (p value)). The size of the circle and colour represents the number of differentially expressed genes in that term. Figures generated using NIPA (available at https://github.com/ADAC-UoN/NIPA). (C) Volcano plots represent the probe sets identified from the transcriptomic analysis. Panel a) Healthy: The red triangles are the differentially expressed probes related to the "Cellular response to stress term" with some representative terms named. In blue are the terms associated with the Nrf-2 pathway in the analysis of healthy AM. Panel b) COPD: The red triangles are the differentially expressed probes related to the "Cellular response to stress" GO term. In blue are the terms associated with NRF2 pathway seen in the Healthy analysis.
285x390mm (300 x 300 DPI)

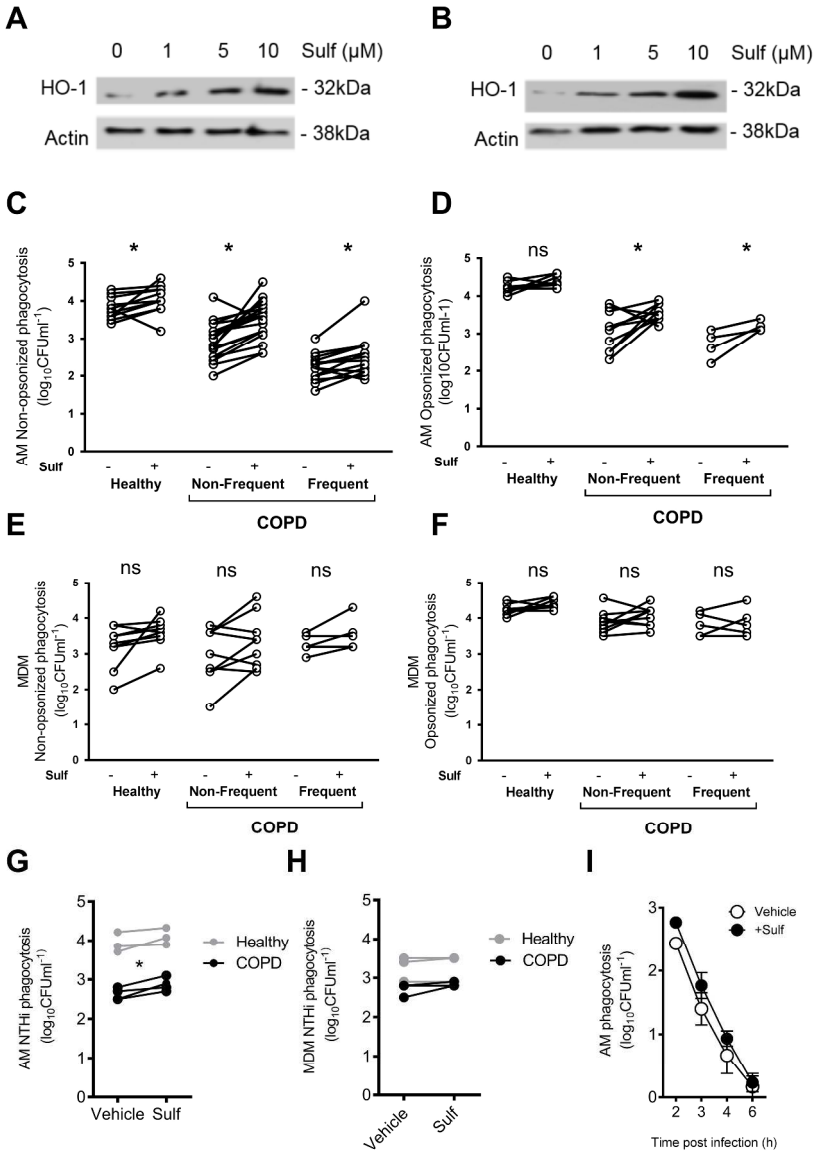

Figure 6. Treatment with the Nrf-2 agonist sulforaphane increases non-opsonic and opsonic phagocytosis in COPD AM but not MDM. (A-B) Alveolar macrophages (AM) and monocyte derived macrophages (MDM)(B) were pre-treated with the designated dose of sulforaphane (Sulf) for 16h, before cells were lysed and probed for expression of heme-oxygenase-1 (HO-1) and actin (n=3). (C-F) AM (C-D) or MDM (E and F) from healthy (H) or COPD non-frequent (NF) or frequent (F) exacerbators were pre-treated with vehicle (Sulf -) or Sulforaphane (Sulf +) for 16 h, before cells were challenged with non-opsonized (C and E) or opsonized (D and F) serotype 14 S. pneumoniae. 4h post-challenge, numbers of intracellular viable bacteria were measured, values for 'n=' for H/COPD-NF/COPD-F; (C) 11/19/14, (D) 8/ 10/4, (E) 9/9/5, (F) 8/9/5, *=p<0.05, paired t-test. (G and H) AM (G) and MDM (H) from COPD patients or healthy (H) donors were pre-treated with sulforaphane before being challenged with non-typeable H. influenzae (NTHi). 4h post challenge the numbers of intracellular viable bacteria were measured, values for 'n=' for H/COPD (G)3/4, (H) 3/3, *=p<0.05, paired t-test. (I) COPD AM were pre-treated with sulforaphane (+Sulf) before being challenged with non-opsonized serotype 14 S. pneumoniae for 4h before extracellular bacteria were killed by the addition of antibiotics. At the designated time post-antibiotics, viable bacteria in duplicate wells were measured to, n=3, no significant difference between vehicle and sulf.

275x385mm (300 x 300 DPI)

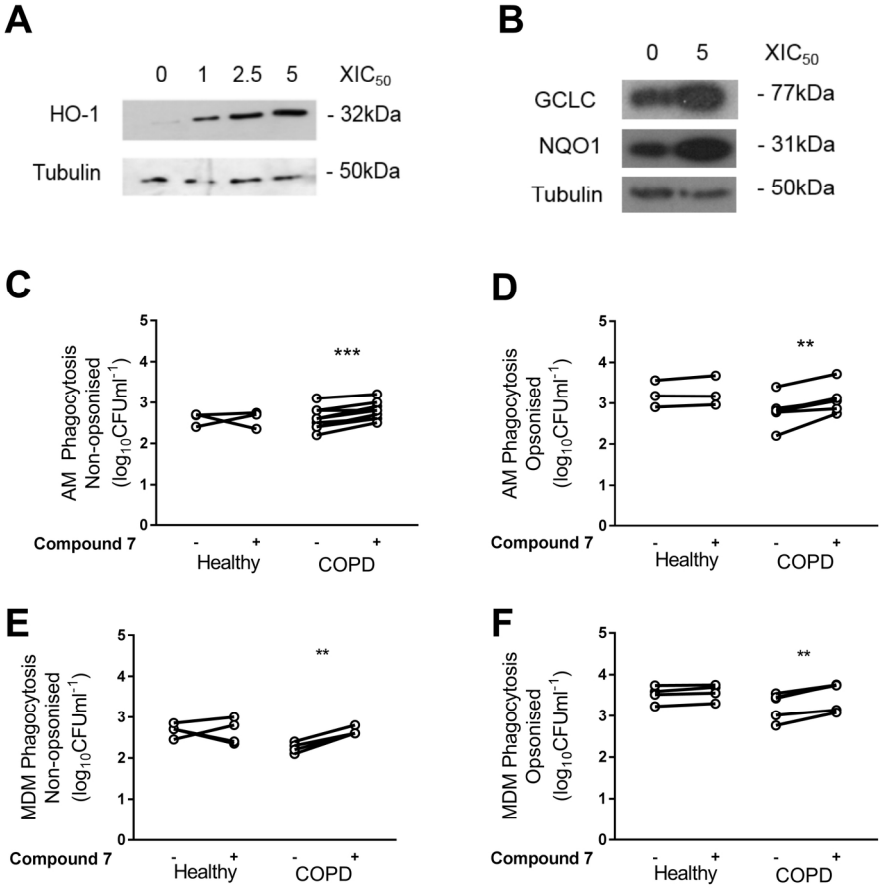

Figure 7. The Nrf-2 agonist compound 7 also increases phagocytosis in COPD AM.
(A and B) COPD monocyte-derived macrophages (MDM) (A), or alveolar macrophages (AM) (B), were pre-treated with the Nrf-2 agonist Compound 7 for 16h at the designated dose, before cells were lysed and a probed for the expression of heme-oxygenase-1 (HO-1), glutamate-cysteine ligase catalytic subunit (GCLC) or NADPH:quinone oxidoreductase 1 (NQO1) by western blot. (C and D) Healthy donor and COPD AM were pre-treated with Compound 7 at 5x IC50 (0.065 M), for 16h before being challenged with opsonized (C), n=3 healthy, n=5 COPD or non-opsonized (D), n=3 healthy, n=10 COPD, serotype 14 S. pneumoniae for 4h, after which numbers of intracellular viable bacteria were assessed, **=p<0.01, paired t-test. (E and F) Healthy donor and COPD MDM were pre-treated with compound 7 and challenged with opsonized (E), or non-opsonized (F), S. pneumoniae as for AM. All n=4, p **=p<0.01, paired t-test.

173x163mm (300 x 300 DPI)

Online Data Supplement

Opsonic phagocytosis in chronic obstructive pulmonary disease is enhanced by Nrf2 agonists.

Martin A. Bewley, Richard C Budd, Eilise Ryan, Joby Cole, Paul Collini, Jennifer Marshall, Umme Kolsum, Gussie Beech, Richard D. Emes, Irina Tcherniaeva, Guy A. M. Berbers, Sarah R. Walmsley, Gavin Donaldson, Jadwiga A. Wedzicha, Iain Kilty, William Rumsey, Yolanda Sanchez, Christopher E. Brightling, Louise E. Donnelly, Peter J. Barnes, Dave Singh, Moira K.B. Whyte and David H. Dockrell, on behalf of COPDMAP.

Supplemental Methods

Macrophage donors: COPD patients were recruited from the UK Medical Research Council (MRC) COPD-MAP consortium, a well-defined clinical cohort of GOLD Stage A-D patients (Table E1). Written approved consent was obtained prior to inclusion in the study as approved by the National Research Ethics Service Committee for Yorkshire and the Humber #11/YH0356 and Greater Manchester South # 06/Q1403/156. Subjects had undergone extensive clinical characterization including, visual analogue symptom (VAS) scores for breathlessness, spirometry and health status assessment. All patients used in the current study had GOLD stage II or III COPD. Controls were healthy ex-smokers (defined as > 6 months smoking cessation) without airflow limitation assessed by spirometry and without symptoms of COPD by screening questionnaire or on clinical examination. Exacerbation frequency was determined by medical history of oral therapy for exacerbation and frequent exacerbators were defined as having had ≥ 2 exacerbations in the preceding 12 months (E1). Bronchoscopies were performed in the stable state, not during exacerbations. Since the yield of samples varied all study participants had an AM sample challenged with non-opsonized bacteria but only approximately three-quarters had sufficient sample to allow challenge with opsonized bacteria. Similarly, not every individual agreed to a blood donation of sufficient yield to allow isolation of monocyte-derived macrophages (MDM). Accordingly, approximately three-quarters of samples had MDM samples for challenge with non-opsonized bacteria and a smaller number enough MDM for challenge with opsonized bacteria. Since the

volume of BAL and the yield of AM varied only approximately half of samples had sufficient numbers for further analysis of sulforaphane.

Assessment scales: Health status and physical activity of the COPD patients was evaluated by a number of validated health-related quality of life (HR-QoL) instruments; the St George's Respiratory Questionnaire (SGRQ)(E2), COPD Assessment Test (CAT)(E3) and Medical Research Council (MRC) dyspnea scale (E4), and with the 6-minute walking distance (6MW) (E5). Scores from these evaluations (with the exception of the MRC dyspnea scale) were then plotted against that patient's phagocytosis rates.

Microbiological assessment:

Sputum quantitative culture was performed according to standard practice (E6) Briefly, the sample was cultured onto suitable agar plates i.e. Columbia blood agar (a general growth media), Chocolate agar (for fastidious bacteria), MacConkey agar (for Gram-negative bacteria), and COBA agar (*Streptococcus* selective supplement). The plates were incubated for 24h to 48h at 37°C and 5% CO_2 and identified accordingly to standard practice using X and V tests (E6). Positive sputum cultures were defined as $>10^5$ colony forming units.

Broncholalveolar lavage (BAL) was also processed for quantitative polymerase chain reaction (qPCR) detection of the common respiratory potentially pathogenic microorganisms (PPM) *H. influenzae*, *M. catarrhalis* and *S. pneumoniae* and for human rhinovirus (RV) as previously described with a positive result defined as $>10^4$ copies/ml (E7). Microbiology results were only available for a subset of donors and relationships were tested against results for sputum or BAL as illustrated.

Microbiology culture of non-typeable Haemophilus influenzae:

Non-typable *H. influenzae (*NCTC 1269) was plated out on chocolate agar overnight before cultures were grown to OD 0.6 in brain heart infusion (BHI) (Oxoid) supplemented with 20% FCS (Lonza), 20 μg/ml NAD (Sigma) and 10 μg/ml Heme (Sigma).

Analysis of pneumococcal antibodies in bronchoalveolar lavage fluid.

Pneumococcal serotype-specific IgG antibody concentrations to 13 pneumococcal serotypes were measured using a fluorescent bead-based multiplex immunoassay (MIA) as described previously by Elberse *et al*. (E8). In short, BAL samples were diluted 1:2 in buffer containing 30 μg/ml cell wall polysaccharide Multi (Statens Serum Institute (SSI), Copenhagen, Denmark) and 5% antibody depleted human serum. An in-house reference serum calibrated on the international 007 standard serum (NIBSC) was diluted twofold in 12 steps and included on each plate together with 3 control sera. All capsular polysaccharides were obtained from the American Type Culture Collection (ATCC, Manassas, VA) except for polysaccharide 7F and 19F from SSI, and 6A which was kindly provided by Pfizer Inc. (New York, NY). For each sample, median fluorescent intensity was converted to IgG concentration (μg/ml) by interpolation from a 5-parameter logistic standard curve. Results were obtained using a Bio-plex 200 system with Bio-plex software (version 6.1, Bio-Rad, UK).

Western blot: Whole cell extracts were isolated using SDS-lysis buffer as described before (E9) and equal protein loaded per lane. Proteins were separated by SDS gel electrophoresis, blotted onto a PVDF membrane, and blocked for 60 min at room

temperature in PBS containing 0.05% Tween with 5% (v/w) skim milk powder. Membranes were incubated overnight at 4°C with antibodies against Exchange protein activated by cAMP 1 (EPAC-1) (Rabbit polyclonal, Abcam, 1:2000), RAP-1 (Rabbit polyclonal, Abcam 1:1000), RAC-1 (Abcam, rabbit polyclonal 1:1000), Heme-oxygenase-1 (HO-1) (Santa Cruz, rabbit polyclonal 1:1000), GCLC (Abcam, rabbit polyclonal 1:1000), NQO1 (Abcam, rabbit polyclonal, 1:1000), tubulin (Abcam, rabbit monoclonal, 1:1000), or actin (Sigma, rabbit polyclonal, 1:2000). Proteins were detected using HRP-conjugated secondary antibodies (1:2000; Dako) and ECL (Amersham Pharmacia). As positive controls for EPAC-1, RAP-1 and RAC-1 MDM were treated in hypoxia (1% O_2 for 6 h).

Bacterial binding: Bacterial binding and internalization was assessed by fluorescence microscopy (Leica DMRB 1000) (E10). At the designated time after infection cells were fixed in 2% paraformaldehyde. Cells were then washed three times in PBS and incubated for 15 min with 100 μg of human IgG_1 (Sigma), then washed three times in PBS and were then incubated with 200 μL PBS containing a 1:20 dilution of serotype specific rabbit anti-pneumococcal antibody (Statens Seruminstitut) for 10 min at 20°C (E11). Wells were then washed and incubated with 200 μL PBS containing a 1:20 dilution of fluorescein isothiocyanate (FITC) conjugated goat anti–rabbit IgG Fc (Dako) and a 1:20 dilution of goat serum. Cells were then washed and incubated with 200 μL PBS containing 0.5 μg/ml 4′6′-diamidino-2-phenylindole (DAPI; Molecular Probes). The number of bound (FITC positive, DAPI positive) and internalized bacteria (FITC negative, DAPI positive) were counted for at least 200 cells per condition (E10). As controls for fluorescence microscopy incubation on ice for 4 h was used as a positive control for adherence, treatment with 100 μg/ml IgG_1 (Sigma)

was used as a negative control for binding and internalization and treatment of bacteria with 20% immune serum as a positive control for internalization.

Cell surface marker expression. For the staining of Fc-gamma receptors, cells were blocked with Human TruStain FcX (Biolegend), specially formulated for blocking FcR without interfering with antibody-mediated specific staining. Cells were blocked for 10 min. at room temperature before being stained with either PE-CD16 (clone 3G8), Alexa Fluor 488-CD32 (clone FUN-2), PE-CD64 (clone 10.1) or corresponding isotype controls (All Biolegend, 5µL/million cells). After staining cells were washed in PBS and analyzed by flow cytometry (BD Biosciences FACSCalibur).

Toxicity assays: Nuclear fragmentation and condensation indicative of apoptosis were detected at 20 h after compound treatment using 4′6′-diamidino-2-phenylindole (DAPI), by reviewers blinded to sample origin. Necrosis was measured by the release of lactate dehydrogenase into supernatants using the Cytotox 96 cell viability kit (Promega), used according to the manufacturer's instructions.

Transcriptomic analysis: Total RNA from alveolar macrophages (AM) of healthy volunteers and COPD patients was extracted using TRI reagent (Sigma) and Direct-Zol^{TM} RNA Miniprep (Zymo research) following the manufacturers protocol. The mRNA was then hybridized onto the Affymetrix® HG-U133 plus 2.0 Array (Affymetrix Inc, Santa Clara). Raw data was analyzed in R (v 3.3.1) using affyPML package to perform background correction using GC Robust Multi-array Average, and quantile normalization. Probes whose expression was in the 20th lowest centile were removed. Differentially expressed genes were identified using Limma to

calculate Moderated t tests and considered significant if adjusted p value <0.05 following Benjamini-Hochberg correction. Genes differentially expressed with respect to infection were tested for overrepresentation of Gene Ontology (GO) terms using a hypergeometric model using GOstats package and figures generated using NIPA (available at https://github.com/ADAC-UoN/NIPA) (FDR <0.05) in R. In addition network analysis shown in Figure E6 was generated using BiNGO software in Cytoscape. The transcriptomic data is available online in the ArrayExpress database at EMBL-EAI .www.ebi.ac.uk/arrayexpress) under accession number E-MTAB-6491.

Supplementary Data

Figure Legends

Figure E1. Relationship between bacterial uptake and exacerbation frequency. Alveolar macrophages (AM) were collected from patients with COPD and were challenged with non-opsonized (NO) or opsonized (O) serotype 14 *S. pneumoniae* for 4 h, before extracellular bacteria were killed by the addition of antibiotics. At the designated time post-antibiotics, viable bacteria in duplicate wells were measured and plotted against exacerbation frequency. 'n' values for NO/O by exacerbation frequency; 0=20/15, 1=7/4, 2=3/2,3=7/74=3/3,5=2/1.

Figure E2. COPD Macrophages show no defect in early-phase bacterial killing. **(A-D)** Alveolar macrophages (AM) (A and B) or monocyte derived macrophages (MDM) were collected from patients with COPD (A and C) or healthy donors (B and D) and were challenged with non-opsonized or opsonized serotype 14 *S. pneumoniae* for 4h, before extracellular bacteria were killed by the addition of antibiotics. At the designated time post-antibiotics, viable bacteria in duplicate wells were measured, n=3, no significant differences between any groups.

Figure E3. COPD alveolar macrophages show defects in uptake of opsonized *S. pneumoniae.* Alveolar macrophages (AM) or monocyte derived macrophages (MDM) were collected from patients with COPD or healthy donors and were challenged with non-opsonized or opsonized serotype 14 *S. pneumoniae* for 4h, before performing fluorescence microscopy to determine adherent (green, continuous arrows) and internalized bacteria (blue, broken arrows. Representative images are shown for fluorescence microscopy of AM (A) and MDM (B) with binding shown in the upper

row and internalization in the lower row. In these experiments incubation on ice was a positive control for binding, IgG_1 treatment to block FcγR was a negative control for both binding and internalization and treatment with 20% immune serum was a positive control for internalization. Pictures are representative of three donors in each condition. **(C-F)** AM (C and E) and MDM (D and F) from healthy and COPD donors (non-frequent or frequent exacerbators) were analyzed to record bacterial binding and internalization under the same conditions by fluorescence microscopy, n=4. * $p<0.05$ by One-way ANOVA.

Figure E4. COPD Macrophages show no defect in Fc-gamma expression or expression of EPAC-1 RAP-1 and RAC-1.

(A-B) Healthy and COPD alveolar macrophages (AM) AM (A) and monocyte derived macrophages (MDM) (B) were analyzed for the expression of either CD16, CD32 or CD64 by flow cytometry, n=3, no significant differences between healthy or COPD. **(C-D)** Healthy or COPD AM from two individual donors (i and ii) were either mock-infected (Spn-) or challenged with serotype 14 *S. pneumoniae* (Spn +). 4h post-challenge cells were lysed and the expression of EPAC-1, RAP1 and RAC1 assessed by western blot. The blot is representative of one of three. (C) Positive controls (+) for EPAC-1, RAP-1 and RAC-1 were hypoxic MDM (as compared to nomoxic MDM (-)).

Figure E5 Pneumococcal antibodies are detectable in broncholaveolar lavage fluid. Bronchoalveolar lavage fluid from 13 healthy and 16 COPD patients was analyzed by multiplex immunoassay for presence of pneumococcal antibodies against 13 *S. pneumoniae* serotypes.

Figure E6. Transcriptional response of AM reveals less differential gene expression in COPD in response to infection. Ontology analysis of Healthy and COPD networks following pneumococcal challenge. The overrepresented terms (calculated with BiNGO software in Cytoscape, FDR <0.05, Hypergeometric clustering) are visualised. The terms for Cellular Response to Stress are highlighted by an arrow in each network.

Figure E7. Treatment with Nrf-2 agonists does not induce apoptosis or necrosis. COPD alveolar macrophages were pre-treated with sulforaphane (+Sulf) or compound 7 for 16h. Cells were then assessed for either necrosis (A) or apoptosis (n=3).

Figure E8. Sulforaphane treatment does not modify Fc-gamma expression in healthy or COPD macrophages. Healthy or COPD alveolar macrophages (AM)(A) or monocyte-derived macrophages (MDM)(B) were pre-treated with sulforaphane (+Sulf) for 16h. Cells were then assessed for expression of CD16, CD32 or CD64 by flow cytometry, n=3.

Table E1: Top differentially regulated gene probes for healthy AM

Healthy AM MI vs *S. pneumoniae*					
Affymetrix probe ID	**logFC**	**q value**	**Entrez**	**Name**	**Gene name**
206407_s_at	8.271748089	0.00017628	6357	CCL13	C-C motif chemokine ligand 13 (CCL13)
205890_s_at	7.470218672	0.000602696	2550	GABBR1	gamma-aminobutyric acid type B receptor subunit 1 (GABBR1)
210873_x_at	7.292943927	0.000639873	200315	APOBEC3A	apolipoprotein B mRNA editing enzyme catalytic subunit 3A (APOBEC3A)
214022_s_at	7.263546468	0.000978422	8519	IFITM1	interferon induced transmembrane protein 1 (IFITM1)
202746_at	6.972741506	0.001622634	9452	ITM2A	integral membrane protein 2A(ITM2A)
203915_at	6.931197241	0.000273857	4283	CXCL9	C-X-C motif chemokine ligand 9 (CXCL9)
208450_at	6.685442365	0.000128955	3957	LGALS2	galectin 2(LGALS2)
209686_at	6.674192457	0.000602696	6285	S100B	S100 calcium binding protein B (S100B)
219836_at	6.530204305	0.000676664	79413	ZBED2	zinc finger BED-type containing 2 (ZBED2)
204563_at	6.474742419	0.000740994	6402	SELL	selectin L (SELL)
209561_at	-5.15603454	0.001764023	7059	THBS3	Thrombospondin 3 (THBS3)
201131_s_at	-5.181392931	0.004915805	999	CDH1	cadherin 1(CDH1)
214366_s_at	-5.330701347	0.029424351	240	ALOX5	arachidonate 5-lipoxygenase (ALOX5)
203716_s_at	-5.351919708	0.002898479	1803	DPP4	dipeptidyl peptidase 4(DPP4)
209728_at	-5.641721827	0.000862231	3126	HLA-DRB4	major histocompatibility complex, class II, DR beta 4 (HLA-DRB4)
211102_s_at	-5.745789792	0.035623081	11027	LILRA2	leukocyte immunoglobulin like receptor A2 (LILRA2)
220784_s_at	-5.86516063	0.003370561	10911	UTS2	urotensin 2 (UTS2)
204364_s_at	-6.03185733	0.003062235	65055	REEP1	receptor accessory protein 1 (REEP1)
219434_at	-6.221508302	0.005872442	54210	TREM1	triggering receptor expressed on myeloid cells 1 (TREM1)
217078_s_at	-6.546933332	0.037935264	11314	CD300A	CD300a molecule (CD300A)

Table E2 Top differentially regulated gene probes for COPD AM

COPD AM MI vs *S. pneumoniae*					
Affymetrix probe ID	**logFC**	**q value**	**Entrez**	**Name**	**Gene name**
204567_s_at	2.014122464	0.048121165	9619	ABCG1	ATP binding cassette subfamily G member 1 (ABCG1)
203315_at	1.979168617	0.031927439	8440	NCK2	NCK adaptor protein 2(NCK2)
219497_s_at	1.853658768	0.029753664	53335	BCL11A	B-cell CLL/lymphoma 11A(BCL11A)
205687_at	1.817410224	0.01483341	56061	UBFD1	ubiquitin family domain containing 1(UBFD1)
201848_s_at	1.816156867	0.036585488	664	BNIP3	BCL2 interacting protein 3(BNIP3)
204972_at	1.811343652	0.043243889	4939	OAS2	2'-5'-oligoadenylate synthetase 2(OAS2)
211113_s_at	1.807154615	0.031256828	9619	ABCG1	ATP Binding Cassette Subfamily G Member 1 (ABCG1)
205552_s_at	1.610119973	0.018262832	4938	OAS1	2'-5'-oligoadenylate synthetase 1(OAS1)
215037_s_at	1.592545166	0.033041465	598	BCL2L1	BCL2 like 1(BCL2L1)
202869_at	1.532562476	0.016248444	4938	OAS1	2'-5'-oligoadenylate synthetase 1(OAS1)
201791_s_at	-1.854527497	0.034527556	1717	DHCR7	7-dehydrocholesterol reductase(DHCR7)
204790_at	-1.864061665	0.01483341	4092	SMAD7	SMAD family member 7(SMAD7)
205403_at	-2.034174738	0.031927439	7850	IL1R2	interleukin 1 receptor type 2(IL1R2)
212282_at	-2.035476503	0.044318817	27346	TMEM97	transmembrane protein 97(TMEM97)
202539_s_at	-2.181882025	0.036240919	3156	HMGCR	3-hydroxy-3-methylglutaryl-CoA reductase(HMGCR)
209218_at	-2.256973195	0.041926617	6713	SQLE	squalene epoxidase(SQLE)
212560_at	-2.257718048	0.038373402	6653	SORL1	sortilin related receptor 1(SORL1)
213577_at	-2.432492887	0.026458227	6713	SQLE	squalene epoxidase(SQLE)
210004_at	-2.510144406	0.015716731	4973	OLR1	oxidized low density lipoprotein receptor 1(OLR1)
207826_s_at	-3.593137708	0.006341014	3399	ID3	inhibitor of DNA binding 3, HLH protein(ID3)

Table E3 Differentially regulated gene probes belonging to GO term Cellular Response to Stress

Healthy				
Affy probe ID	**logFC**	**q value**	**Name**	**Gene name**
209686_at	6.6742	0.0006	S100B	S100 calcium binding protein B (S100B)
226315_at	1.3878	0.0007	ZNF830	zinc finger protein 830 (ZNF830)
207785_s_at	1.2269	0.0007	RBPJ	recombination signal binding protein for immunoglobulin kappa J region (RBPJ)
205904_at	-1.9848	0.0008	MICA	MHC class I polypeptide-related sequence A (MICA)
205967_at	3.6889	0.0008	HIST1H4C	histone cluster 1 H4 family member c (HIST1H4C)
204224_s_at	5.3079	0.0008	GCH1	GTP cyclohydrolase 1 (GCH1)
200878_at	-1.6743	0.0009	EPAS1	endothelial PAS domain protein 1 (EPAS1)
238831_at	-2.4749	0.0010	TMEM33	transmembrane protein 33 (TMEM33)
217550_at	-2.8103	0.0010	ATF6	activating transcription factor 6 (ATF6)
204279_at	4.1151	0.0010	PSMB9	proteasome subunit beta 9(PSMB9)
218041_x_at	-1.8503	0.0011	SLC38A2	solute carrier family 38 member 2 (SLC38A2)
204466_s_at	-5.0755	0.0011	SNCA	synuclein alpha (SNCA)
202503_s_at	5.5584	0.0011	PCLAF	PCNA clamp associated factor (PCLAF)
227228_s_at	4.2187	0.0012	CCDC88C	coiled-coil domain containing 88C (CCDC88C)
203611_at	1.5877	0.0013	TERF2	telomeric repeat binding factor 2 (TERF2)
209959_at	6.1518	0.0014	NR4A3	nuclear receptor subfamily 4 group A member 3 (NR4A3)
206488_s_at	-2.1956	0.0014	CD36	CD36 molecule (CD36)
208808_s_at	3.9025	0.0014	HMGB2	high mobility group box 2 (HMGB2)
221700_s_at	1.3430	0.0015	UBA52	ubiquitin A-52 residue ribosomal protein fusion product 1 (UBA52)
224833_at	4.4827	0.0015	ETS1	ETS proto-oncogene 1, transcription factor (ETS1)
220924_s_at	-1.9034	0.0015	SLC38A2	solute carrier family 38 member 2 (SLC38A2)
209555_s_at	-2.4553	0.0015	CD36	CD36 molecule(CD36)
1558549_s_at	-4.5040	0.0015	VNN1	vanin 1 (VNN1)
226248_s_at	4.0831	0.0015	KIAA1324	KIAA1324 (KIAA1324)
200016_x_at	1.1062	0.0015	HNRNPA1	heterogeneous nuclear

				ribonucleoprotein A1 (HNRNPA1)
228999_at	2.8726	0.0015	CHD2	chromodomain helicase DNA binding protein 2 (CHD2)
225655_at	3.9528	0.0015	UHRF1	ubiquitin like with PHD and ring finger domains 1 (UHRF1)
201762_s_at	1.8409	0.0015	PSME2	proteasome activator subunit 2 (PSME2)
213356_x_at	1.1694	0.0015	HNRNPA1	heterogeneous nuclear ribonucleoprotein A1 (HNRNPA1)
202644_s_at	2.7125	0.0015	TNFAIP3	TNF alpha induced protein 3 (TNFAIP3)
224847_at	1.6661	0.0015	CDK6	cyclin dependent kinase 6 (CDK6)
234000_s_at	-2.0247	0.0015	HACD3	3-hydroxyacyl-CoA dehydratase 3 (HACD3)
209304_x_at	1.6855	0.0016	GADD45B	growth arrest and DNA damage inducible beta (GADD45B)
200814_at	2.1663	0.0016	PSME1	proteasome activator subunit 1 (PSME1)
203510_at	-4.5338	0.0016	MET	MET proto-oncogene, receptor tyrosine kinase (MET)
238653_at	1.3389	0.0016	LRIG2	leucine rich repeats and immunoglobulin like domains 2 (LRIG2)
220384_at	3.4506	0.0016	NME8	NME/NM23 family member 8(NME8)
212634_at	-1.3049	0.0016	UFL1	UFM1 specific ligase 1 (UFL1)
205197_s_at	-4.3706	0.0016	ATP7A	ATPase copper transporting alpha (ATP7A)
236341_at	5.7210	0.0016	CTLA4	cytotoxic T-lymphocyte associated protein 4 (CTLA4)
203553_s_at	-1.5803	0.0017	MAP4K5	mitogen-activated protein kinase kinase kinase kinase 5 (MAP4K5)
220949_s_at	2.1958	0.0017	C7orf49	chromosome 7 open reading frame 49 (C7orf49)
203445_s_at	1.3278	0.0017	CTDSP2	CTD small phosphatase 2 (CTDSP2)
207113_s_at	3.9122	0.0017	TNF	tumor necrosis factor (TNF)
202153_s_at	1.2330	0.0017	NUP62	nucleoporin 62 (NUP62)
37145_at	5.7873	0.0017	GNLY	Granulysin (GNLY)
210426_x_at	2.9696	0.0018	RORA	RAR related orphan receptor A (RORA)
217373_x_at	-1.5002	0.0018	MDM2	MDM2 proto-oncogene (MDM2)
217807_s_at	2.6021	0.0018	NOP53	NPR2-like, GATOR1 complex subunit (NPRL2)
218197_s_at	-1.8142	0.0018	OXR1	oxidation resistance 1 (OXR1)
202181_at	1.0875	0.0019	SUSD6	sushi domain containing 6 (SUSD6)
226991_at	4.1911	0.0019	NFATC2	nuclear factor of activated T-cells 2 (NFATC2)

200944_s_at	1.6260	0.0019	HMGN1	high mobility group nucleosome binding domain 1 (HMGN1)
205965_at	1.2119	0.0019	BATF	basic leucine zipper ATF-like transcription factor (BATF)
215223_s_at	2.2428	0.0019	SOD2	superoxide dismutase 2, mitochondrial (SOD2)
226032_at	1.2471	0.0019	CASP2	caspase 2 (CASP2)
39248_at	3.9050	0.0019	AQP3	aquaporin 3 (Gill blood group) (AQP3)
209033_s_at	1.1523	0.0020	DYRK1A	dual specificity tyrosine phosphorylation regulated kinase 1A (DYRK1A)
207819_s_at	-3.4365	0.0020	ABCB4	ATP binding cassette subfamily B member 4 (ABCB4)
207072_at	3.6333	0.0020	IL18RAP	interleukin 18 receptor accessory protein (IL18RAP)
225053_at	1.2457	0.0021	CNOT7	CCR4-NOT transcription complex subunit 7 (CNOT7)
205905_s_at	-2.3166	0.0022	MICA	MHC class I polypeptide-related sequence A (MICA)
200019_s_at	1.9603	0.0022	SYVN1	synoviolin 1(SYVN1)
210479_s_at	3.2586	0.0022	RORA	RAR related orphan receptor A (RORA)
226682_at	3.2016	0.0022	RORA	RAR related orphan receptor A (RORA)
200896_x_at	1.4362	0.0022	HDGF	hepatoma-derived growth factor (HDGF)
205495_s_at	5.6931	0.0023	GNLY	Granulysin (GNLY)
203984_s_at	1.4089	0.0024	CASP9	caspase 9 (CASP9)
48531_at	1.7755	0.0024	TNIP2	TNFAIP3 interacting protein 2 (TNIP2)
224162_s_at	2.5697	0.0024	FBXO31	F-box protein 31 (FBXO31)
206235_at	-2.0013	0.0024	LIG4	DNA ligase 4 (LIG4)
1552703_s_at	2.1788	0.0025	CARD16	caspase recruitment domain family member 16 (CARD16)
200879_s_at	-3.4515	0.0025	EPAS1	endothelial PAS domain protein 1 (EPAS1)
204908_s_at	3.1879	0.0025	BCL3	B-cell CLL/lymphoma 3 (BCL3)
212345_s_at	-1.1560	0.0026	CREB3L2	cAMP responsive element binding protein 3 like 2 (CREB3L2)
231927_at	-1.1676	0.0026	ATF6	activating transcription factor 6 (ATF6)
225606_at	3.8722	0.0027	BCL2L11	BCL2 like 11 (BCL2L11)
202061_s_at	-1.5678	0.0027	SEL1L	SEL1L ERAD E3 ligase adaptor subunit (SEL1L)
221473_x_at	-1.3400	0.0028	SERINC3	serine incorporator 3 (SERINC3)

227931_at	-1.6590	0.0028	INO80D	INO80 complex subunit D (INO80D)
209294_x_at	-1.2891	0.0028	TNFRSF10B	TNF receptor superfamily member 10b (TNFRSF10B)
222982_x_at	-1.4575	0.0028	SLC38A2	solute carrier family 38 member 2 (SLC38A2)
216264_s_at	-2.9882	0.0028	LAMB2	laminin subunit beta 2 (LAMB2)
209239_at	2.4615	0.0028	NFKB1	nuclear factor kappa B subunit 1 (NFKB1)
203418_at	3.2141	0.0029	CCNA2	cyclin A2 (CCNA2)
203628_at	-2.2550	0.0029	IGF1R	insulin like growth factor 1 receptor (IGF1R)
224731_at	1.3281	0.0029	HMGB1	high mobility group box 1 (HMGB1)
201830_s_at	3.1156	0.0029	NET1	neuroepithelial cell transforming 1 (NET1)
200797_s_at	1.4190	0.0029	MCL1	BCL2 family apoptosis regulator (MCL1)
202243_s_at	1.3195	0.0030	PSMB4	proteasome subunit beta 4 (PSMB4)
205180_s_at	-1.4435	0.0030	ADAM8	ADAM metallopeptidase domain 8 (ADAM8)
223278_at	3.0753	0.0030	GJB2	gap junction protein beta 2 (GJB2)
205179_s_at	-2.3409	0.0030	ADAM8	ADAM metallopeptidase domain 8 (ADAM8)
207827_x_at	-4.1027	0.0030	SNCA	synuclein alpha (SNCA)
204318_s_at	1.8301	0.0030	GTSE1	G2 and S-phase expressed 1 (GTSE1)
203460_s_at	-1.0503	0.0031	PSEN1	presenilin 1 (PSEN1)
222404_x_at	-1.9551	0.0031	HACD3	3-hydroxyacyl-CoA dehydratase 3 (HACD3)
218172_s_at	-1.2967	0.0031	DERL1	derlin 1 (DERL1)
203214_x_at	3.8980	0.0032	CDK1	cyclin dependent kinase 1 (CDK1)
225924_at	-2.2151	0.0032	FNIP2	folliculin interacting protein 2 (FNIP2)
207574_s_at	2.0552	0.0033	GADD45B	growth arrest and DNA damage inducible beta (GADD45B)
200642_at	1.1138	0.0033	SOD1	superoxide dismutase 1, soluble (SOD1)
231736_x_at	-1.0800	0.0033	MGST1	microsomal glutathione S-transferase 1 (MGST1)
211327_x_at	-1.4604	0.0034	HFE	Hemochromatosis (HFE)
211769_x_at	-1.4732	0.0034	SERINC3	serine incorporator 3 (SERINC3)
214280_x_at	1.5241	0.0034	HNRNPA1	heterogeneous nuclear ribonucleoprotein A1 (HNRNPA1)
207347_at	2.6408	0.0035	ERCC6	ERCC excision repair 6, chromatin remodeling factor (ERCC6)
218738_s_at	1.6571	0.0036	RNF138	ring finger protein 138 (RNF138)
205550_s_at	-1.2715	0.0036	BABAM2	BRISC and BRCA1 A complex member

				2 (BABAM2)
201531_at	1.7311	0.0036	ZFP36	ZFP36 ring finger protein (ZFP36)
228766_at	-2.2228	0.0036	CD36	CD36 molecule (CD36)
1553402_a_at	-2.7985	0.0036	HFE	hemochromatosis(HFE)
226460_at	-2.5348	0.0037	FNIP2	folliculin interacting protein 2 (FNIP2)
208760_at	2.7396	0.0037	UBE2I	ubiquitin conjugating enzyme E2 I (UBE2I)
219625_s_at	-2.1514	0.0038	COL4A3BP	collagen type IV alpha 3 binding protein (COL4A3BP)
236266_at	1.6067	0.0038	RORA	RAR related orphan receptor A (RORA)
210793_s_at	2.7189	0.0038	NUP98	nucleoporin 98 (NUP98)
209503_s_at	1.3352	0.0038	PSMC5	proteasome 26S subunit, ATPase 5 (PSMC5)
205590_at	2.6805	0.0039	RASGRP1	RAS guanyl releasing protein 1 (RASGRP1)
201272_at	-1.4230	0.0039	AKR1B1	aldo-keto reductase family 1 member B (AKR1B1)
204533_at	4.9554	0.0039	CXCL10	C-X-C motif chemokine ligand 10 (CXCL10)
218069_at	1.3613	0.0040	DCTPP1	dCTP pyrophosphatase 1 (DCTPP1)
218403_at	1.1052	0.0041	TRIAP1	TP53 regulated inhibitor of apoptosis 1 (TRIAP1)
201812_s_at	1.6611	0.0041	TOMM7	translocase of outer mitochondrial membrane 7 (TOMM7)
204467_s_at	-2.2398	0.0041	SNCA	synuclein alpha (SNCA)
225160_x_at	-3.3167	0.0041	MDM2	MDM2 proto-oncogene (MDM2)
222432_s_at	-1.6379	0.0041	CCDC47	coiled-coil domain containing 47 (CCDC47)
211332_x_at	-1.4186	0.0041	HFE	Hemochromatosis (HFE)
211546_x_at	-3.0292	0.0041	SNCA	synuclein alpha (SNCA)
215997_s_at	-1.1916	0.0041	CUL4B	cullin 4B (CUL4B)
1554462_a_at	-1.8792	0.0041	DNAJB9	DnaJ heat shock protein family (Hsp40) member B9 (DNAJB9)
201737_s_at	-2.9591	0.0042	MARCH6	membrane associated ring-CH-type finger 6 (MARCH6)
209112_at	2.9984	0.0042	CDKN1B	cyclin dependent kinase inhibitor 1B (CDKN1B)
222763_s_at	1.7050	0.0042	WDR33	WD repeat domain 33 (WDR33)
224918_x_at	-1.0379	0.0042	MGST1	microsomal glutathione S-transferase 1 (MGST1)
201649_at	2.3181	0.0043	UBE2L6	ubiquitin conjugating enzyme E2 L6 (UBE2L6)
201345_s_at	1.1380	0.0044	UBE2D2	ubiquitin conjugating enzyme E2 D2 (UBE2D2)

200943_at	1.5113	0.0045	HMGN1	high mobility group nucleosome binding domain 1 (HMGN1)
204009_s_at	1.2088	0.0045	KRAS	KRAS proto-oncogene, GTPase(KRAS)
229290_at	-3.4747	0.0045	DAPL1	death associated protein like 1 (DAPL1)
213226_at	2.8150	0.0045	CCNA2	cyclin A2(CCNA2)
225135_at	2.7524	0.0046	SIN3A	SIN3 transcription regulator family member A (SIN3A)
213095_x_at	2.0801	0.0046	AIF1	allograft inflammatory factor 1 (AIF1)
226507_at	1.0012	0.0046	PAK1	p21 (RAC1) activated kinase 1 (PAK1)
225763_at	3.3710	0.0047	RCSD1	RCSD domain containing 1 (RCSD1)
206087_x_at	-1.5647	0.0047	HFE	Hemochromatosis (HFE)
238005_s_at	1.9612	0.0047	SIN3A	SIN3 transcription regulator family member A (SIN3A)
212240_s_at	1.6710	0.0048	PIK3R1	phosphoinositide-3-kinase regulatory subunit 1 (PIK3R1)
218609_s_at	1.9037	0.0048	NUDT2	nudix hydrolase 2 (NUDT2)
228442_at	3.9652	0.0048	NFATC2	nuclear factor of activated T-cells 2 (NFATC2)
204959_at	2.5601	0.0048	MNDA	myeloid cell nuclear differentiation antigen (MNDA)
202063_s_at	-2.2928	0.0049	SEL1L	SEL1L ERAD E3 ligase adaptor subunit (SEL1L)
220987_s_at	2.5271	0.0049	NUAK2	NUAK family kinase 2 (NUAK2)
203379_at	1.1304	0.0049	RPS6KA1	ribosomal protein S6 kinase A1 (RPS6KA1)
232064_at	-1.1974	0.0050	FER	FER tyrosine kinase (FER)
208827_at	1.2966	0.0050	PSMB6	proteasome subunit beta 6 (PSMB6)
202164_s_at	1.0752	0.0051	CNOT8	CCR4-NOT transcription complex subunit 8 (CNOT8)
204798_at	4.2929	0.0052	MYB	MYB proto-oncogene, transcription factor (MYB)
209619_at	2.5167	0.0052	CD74	CD74 molecule (CD74)
225838_at	1.2063	0.0053	EPC2	enhancer of polycomb homolog 2 (EPC2)
201829_at	2.3673	0.0053	NET1	neuroepithelial cell transforming 1 (NET1)
226295_at	1.5538	0.0053	ITFG2	integrin alpha FG-GAP repeat containing 2 (ITFG2)
203525_s_at	-1.5824	0.0053	APC	APC, WNT signaling pathway regulator (APC)
201202_at	2.0012	0.0054	PCNA	proliferating cell nuclear antigen (PCNA)
230425_at	-1.4333	0.0054	EPHB1	EPH receptor B1 (EPHB1)
214084_x_at	2.9014	0.0054	NCF1	neutrophil cytosolic factor 1 (NCF1)

200798_x_at	1.4244	0.0055	MCL1	BCL2 family apoptosis regulator (MCL1)
202724_s_at	1.5573	0.0055	FOXO1	forkhead box O1 (FOXO1)
209901_x_at	2.1444	0.0055	AIF1	allograft inflammatory factor 1 (AIF1)
212676_at	-1.7643	0.0056	NF1	neurofibromin 1 (NF1)
225252_at	1.0819	0.0056	SRXN1	sulfiredoxin 1 (SRXN1)
202306_at	1.6480	0.0056	POLR2G	RNA polymerase II subunit G (POLR2G)
218465_at	-1.3747	0.0057	TMEM33	transmembrane protein 33 (TMEM33)
1552263_at	2.1817	0.0057	MAPK1	mitogen-activated protein kinase 1 (MAPK1)
201250_s_at	-1.3782	0.0057	SLC2A1	solute carrier family 2 member 1 (SLC2A1)
225364_at	1.1928	0.0057	STK4	serine/threonine kinase 4 (STK4)
205733_at	3.3307	0.0057	BLM	Bloom syndrome RecQ like helicase (BLM)
1552701_a_at	2.8111	0.0058	CARD16	caspase recruitment domain family member 16 (CARD16)
206271_at	1.9634	0.0058	TLR3	toll like receptor 3(TLR3)
218250_s_at	1.3350	0.0058	CNOT7	CCR4-NOT transcription complex subunit 7 (CNOT7)
215051_x_at	1.8362	0.0058	AIF1	allograft inflammatory factor 1 (AIF1)
203213_at	4.7116	0.0059	CDK1	cyclin dependent kinase 1 (CDK1)
228528_at	1.4066	0.0059	MIR29B2	microRNA 29b-2 (MIR29B2)
201292_at	4.6705	0.0059	TOP2A	topoisomerase (DNA) II alpha (TOP2A)
221666_s_at	2.1472	0.0060	PYCARD	PYD and CARD domain containing (PYCARD)
202659_at	2.7855	0.0060	PSMB10	proteasome subunit beta 10 (PSMB10)
229119_s_at	1.7095	0.0061	ZSWIM7	zinc finger SWIM-type containing 7 (ZSWIM7)
202786_at	3.3043	0.0062	STK39	serine/threonine kinase 39 (STK39)
225196_s_at	1.8963	0.0062	MRPS26	mitochondrial ribosomal protein S26 (MRPS26)
205844_at	-3.9550	0.0063	VNN1	vanin 1 (VNN1)
230285_at	2.8850	0.0063	SVIP	small VCP interacting protein (SVIP)
205960_at	-2.4753	0.0064	PDK4	pyruvate dehydrogenase kinase 4 (PDK4)
222903_s_at	-1.1056	0.0064	CPEB1	cytoplasmic polyadenylation element binding protein 1 (CPEB1)
225837_at	3.3714	0.0064	RHNO1	RAD9-HUS1-RAD1 interacting nuclear orphan 1 (RHNO1)
224734_at	1.6224	0.0064	HMGB1	high mobility group box 1 (HMGB1)

1552798_a_at	-1.8891	0.0065	TLR4	toll like receptor 4 (TLR4)
1565162_s_at	-1.5077	0.0065	MGST1	microsomal glutathione S-transferase 1 (MGST1)
224700_at	-1.1908	0.0067	STT3B	STT3B, catalytic subunit of the oligosaccharyltransferase complex (STT3B)
212955_s_at	1.1254	0.0067	POLR2I	RNA polymerase II subunit I (POLR2I)
238311_at	-2.1781	0.0068	UFL1	UFM1 specific ligase 1 (UFL1)
225344_at	1.3596	0.0068	NCOA7	nuclear receptor coactivator 7 (NCOA7)
230127_at	-3.0843	0.0068	MIR222	microRNA 222 (MIR222)
230127_at	-3.0843	0.0068	MIR221	microRNA 221 (MIR221)
222642_s_at	-2.1825	0.0069	TMEM33	transmembrane protein 33 (TMEM33)
208878_s_at	1.3135	0.0069	PAK2	p21 (RAC1) activated kinase 2 (PAK2)
226547_at	1.5238	0.0070	KAT6A	lysine acetyltransferase 6A (KAT6A)
222569_at	-1.4495	0.0070	UGGT1	UDP-glucose glycoprotein glucosyltransferase 1 (UGGT1)
225099_at	1.2510	0.0070	FBXO45	F-box protein 45 (FBXO45)
243869_at	1.0727	0.0070	CCDC88C	coiled-coil domain containing 88C (CCDC88C)
201589_at	1.4712	0.0071	SMC1A	structural maintenance of chromosomes 1A (SMC1A)
1559946_s_at	1.5700	0.0071	RUVBL2	RuvB like AAA ATPase 2 (RUVBL2)
239328_at	2.0917	0.0071	RCSD1	RCSD domain containing 1 (RCSD1)
1555808_a_at	-3.1544	0.0071	EXD2	exonuclease 3'-5' domain containing 2 (EXD2)
221521_s_at	3.2555	0.0073	GINS2	GINS complex subunit 2 (GINS2)
201236_s_at	2.2976	0.0074	BTG2	BTG anti-proliferation factor 2 (BTG2)
204751_x_at	-1.9213	0.0076	DSC2	desmocollin 2 (DSC2)
212022_s_at	2.7573	0.0076	MKI67	marker of proliferation Ki-67 (MKI67)
227545_at	1.6685	0.0077	BARD1	BRCA1 associated RING domain 1 (BARD1)
225492_at	-1.3006	0.0078	TMEM33	transmembrane protein 33 (TMEM33)
224778_s_at	-1.7326	0.0078	TAOK1	TAO kinase 1 (TAOK1)
225207_at	-3.1276	0.0079	PDK4	pyruvate dehydrogenase kinase 4 (PDK4)
201489_at	1.2158	0.0081	PPIF	peptidylprolyl isomerase F (PPIF)
201174_s_at	1.3594	0.0081	TERF2IP	TERF2 interacting protein (TERF2IP)
228650_at	1.5387	0.0081	POLR2D	RNA polymerase II subunit D (POLR2D)
226170_at	1.1691	0.0082	EYA3	EYA transcriptional coactivator and phosphatase 3 (EYA3)

201400_at	1.3774	0.0082	PSMB3	proteasome subunit beta 3 (PSMB3)
200651_at	1.3886	0.0082	RACK1	receptor for activated C kinase 1 (RACK1)
203415_at	1.2492	0.0083	PDCD6	programmed cell death 6 (PDCD6)
211330_s_at	-2.8336	0.0083	HFE	Hemochromatosis (HFE)
224666_at	1.8143	0.0084	NSMCE1	NSE1 homolog, SMC5-SMC6 complex component (NSMCE1)
223243_s_at	-1.9093	0.0084	EDEM3	ER degradation enhancing alpha-mannosidase like protein 3 (EDEM3)
223229_at	2.5335	0.0085	UBE2T	ubiquitin conjugating enzyme E2 T (UBE2T)
223466_x_at	-1.9873	0.0085	COL4A3BP	collagen type IV alpha 3 binding protein (COL4A3BP)
212685_s_at	-1.1941	0.0085	TBL2	transducin beta like 2 (TBL2)
206686_at	-1.6488	0.0086	PDK1	pyruvate dehydrogenase kinase 1 (PDK1)
212099_at	2.9696	0.0087	RHOB	ras homolog family member B (RHOB)
210218_s_at	1.7682	0.0087	SP100	SP100 nuclear antigen (SP100)
204286_s_at	2.7352	0.0087	PMAIP1	phorbol-12-myristate-13-acetate-induced protein 1 (PMAIP1)
1558143_a_at	2.4384	0.0088	BCL2L11	BCL2 like 11 (BCL2L11)
202213_s_at	-1.4501	0.0089	CUL4B	cullin 4B (CUL4B)
225922_at	-1.5750	0.0090	FNIP2	folliculin interacting protein 2 (FNIP2)
203185_at	1.0784	0.0091	RASSF2	Ras association domain family member 2 (RASSF2)
208510_s_at	-1.2364	0.0091	PPARG	peroxisome proliferator activated receptor gamma (PPARG)
209230_s_at	-2.0579	0.0092	NUPR1	nuclear protein 1, transcriptional regulator (NUPR1)
225123_at	2.7206	0.0093	SESN3	sestrin 3 (SESN3)
203241_at	1.2243	0.0094	UVRAG	UV radiation resistance associated (UVRAG)
203719_at	1.3789	0.0094	ERCC1	ERCC excision repair 1, endonuclease non-catalytic subunit (ERCC1)
200039_s_at	1.1403	0.0095	PSMB2	proteasome subunit beta 2 (PSMB2)
203322_at	1.4707	0.0095	ADNP2	ADNP homeobox 2 (ADNP2)
242352_at	1.7493	0.0096	NIPBL	NIPBL, cohesin loading factor (NIPBL)
216944_s_at	-1.3244	0.0097	ITPR1	inositol 1,4,5-trisphosphate receptor type 1 (ITPR1)
214647_s_at	-3.1687	0.0097	HFE	Hemochromatosis (HFE)
200017_at	1.2467	0.0099	RPS27A	ribosomal protein S27a (RPS27A)
218505_at	1.2044	0.0099	WDR59	WD repeat domain 59 (WDR59)
206554_x_at	2.0061	0.0100	SETMAR	SET domain and mariner transposase

				fusion gene (SETMAR)
212678_at	-1.6486	0.0100	NF1	neurofibromin 1 (NF1)
214352_s_at	1.1980	0.0100	KRAS	KRAS proto-oncogene, GTPase (KRAS)
213682_at	1.6406	0.0101	NUP50	nucleoporin 50 (NUP50)
209139_s_at	1.3821	0.0102	PRKRA	protein activator of interferon induced protein kinase EIF2AK2 (PRKRA)
202516_s_at	-1.4618	0.0102	DLG1	discs large MAGUK scaffold protein 1 (DLG1)
208988_at	1.4209	0.0103	KDM2A	lysine demethylase 2A (KDM2A)
242751_at	-1.6397	0.0103	PRDX6	peroxiredoxin 6 (PRDX6)
242197_x_at	-1.6963	0.0104	CD36	CD36 molecule (CD36)
218979_at	1.3828	0.0104	RMI1	RecQ mediated genome instability 1 (RMI1)
228281_at	3.1577	0.0104	DDIAS	DNA damage induced apoptosis suppressor (DDIAS)
209539_at	1.1853	0.0105	ARHGEF6	Rac/Cdc42 guanine nucleotide exchange factor 6 (ARHGEF6)
209111_at	1.9760	0.0106	RNF5	ring finger protein 5 (RNF5)
201459_at	1.2695	0.0107	RUVBL2	RuvB like AAA ATPase 2 (RUVBL2)
225227_at	1.6918	0.0107	SKIL	SKI like proto-oncogene (SKIL)
204566_at	1.1329	0.0107	PPM1D	protein phosphatase, Mg2+/Mn2+ dependent 1D (PPM1D)
212594_at	1.5576	0.0107	PDCD4	programmed cell death 4 (neoplastic transformation inhibitor) (PDCD4)
202539_s_at	-1.3987	0.0107	HMGCR	3-hydroxy-3-methylglutaryl-CoA reductase (HMGCR)
211566_x_at	-1.0153	0.0108	BABAM2	BRISC and BRCA1 A complex member 2 (BABAM2)
232160_s_at	2.1464	0.0109	TNIP2	TNFAIP3 interacting protein 2 (TNIP2)
203246_s_at	1.2654	0.0110	NPRL2	nuclear receptor subfamily 4 group A member 2 (NR4A2)
209507_at	2.0217	0.0113	RPA3	replication protein A3 (RPA3)
212106_at	-1.4907	0.0113	FAF2	Fas associated factor family member 2 (FAF2)
202413_s_at	1.4013	0.0113	USP1	ubiquitin specific peptidase 1 (USP1)
211329_x_at	-1.4858	0.0113	HFE	Hemochromatosis (HFE)
204780_s_at	1.2127	0.0114	FAS	Fas cell surface death receptor (FAS)
204127_at	1.9537	0.0115	RFC3	replication factor C subunit 3 (RFC3)
226760_at	-1.1058	0.0116	MBTPS2	membrane bound transcription factor peptidase, site 2 (MBTPS2)
202721_s_at	-1.2262	0.0117	GFPT1	glutamine--fructose-6-phosphate transaminase 1 (GFPT1)

223465_at	-1.4203	0.0117	COL4A3BP	collagen type IV alpha 3 binding protein (COL4A3BP)
222476_at	1.4670	0.0120	CNOT6	CCR4-NOT transcription complex subunit 6 (CNOT6)
200803_s_at	-1.1438	0.0121	TMBIM6	transmembrane BAX inhibitor motif containing 6 (TMBIM6)
210148_at	-2.2230	0.0121	HIPK3	homeodomain interacting protein kinase 3 (HIPK3)
201241_at	-1.0058	0.0122	DDX1	DEAD-box helicase 1 (DDX1)
238420_at	-1.8221	0.0123	TAOK1	TAO kinase 1 (TAOK1)
233421_s_at	-1.0662	0.0124	NUP133	nucleoporin 133 (NUP133)
203554_x_at	2.4385	0.0125	PTTG1	pituitary tumor-transforming 1(PTTG1)
222600_s_at	-2.0859	0.0125	UBA6	ubiquitin like modifier activating enzyme 6 (UBA6)
201161_s_at	1.1163	0.0126	YBX3	Y-box binding protein 3 (YBX3)
202064_s_at	-2.0579	0.0126	SEL1L	SEL1L ERAD E3 ligase adaptor subuni t(SEL1L)
224780_at	1.4898	0.0127	RBM17	RNA binding motif protein 17 (RBM17)
204484_at	1.1172	0.0128	PIK3C2B	phosphatidylinositol-4-phosphate 3-kinase catalytic subunit type 2 beta (PIK3C2B)
205386_s_at	-1.6688	0.0128	MDM2	MDM2 proto-oncogene (MDM2)
219035_s_at	1.7347	0.0129	RNF34	ring finger protein 34 (RNF34)
218117_at	1.1157	0.0130	RBX1	ring-box 1 (RBX1)
222494_at	1.3845	0.0130	FOXN3	forkhead box N3 (FOXN3)
213137_s_at	2.5706	0.0131	PTPN2	protein tyrosine phosphatase, non-receptor type 2 (PTPN2)
219007_at	1.4048	0.0131	NUP43	nucleoporin 43 (NUP43)
231769_at	1.7185	0.0131	FBXO6	F-box protein 6 (FBXO6)
209341_s_at	1.1861	0.0132	IKBKB	inhibitor of kappa light polypeptide gene enhancer in B-cells, kinase beta (IKBKB)
218845_at	1.2237	0.0132	DUSP22	dual specificity phosphatase 22 (DUSP22)
208744_x_at	-1.5729	0.0134	HSPH1	heat shock protein family H (Hsp110) member 1 (HSPH1)
226157_at	1.0799	0.0135	TFDP2	transcription factor Dp-2 (TFDP2)
204285_s_at	2.2882	0.0136	PMAIP1	phorbol-12-myristate-13-acetate-induced protein 1 (PMAIP1)
204781_s_at	1.4655	0.0136	FAS	Fas cell surface death receptor (FAS)
224972_at	1.3415	0.0137	ROMO1	reactive oxygen species modulator 1 (ROMO1)
208875_s_at	2.3841	0.0140	PAK2	p21 (RAC1) activated kinase 2 (PAK2)

1294_at	2.3040	0.0141	UBA7	ubiquitin like modifier activating enzyme 7 (UBA7)
206181_at	3.7115	0.0142	SLAMF1	signaling lymphocytic activation molecule family member 1 (SLAMF1)
218498_s_at	-1.4255	0.0142	ERO1A	endoplasmic reticulum oxidoreductase 1 alpha (ERO1A)
216248_s_at	3.3321	0.0142	NR4A2	nuclear receptor subfamily 4 group A member 2 (NR4A2)
203062_s_at	1.8885	0.0142	MDC1	mediator of DNA damage checkpoint 1 (MDC1)
204767_s_at	1.9439	0.0143	FEN1	flap structure-specific endonuclease 1 (FEN1)
201370_s_at	2.1983	0.0144	CUL3	cullin 3 (CUL3)
226521_s_at	1.5128	0.0144	FAM175A	double-strand break repairvia (FAM175A)
228333_at	1.3747	0.0145	ZEB2	zinc finger E-box binding homeobox 2 (ZEB2)
1558080_s_at	-3.8846	0.0146	DNAJC3	DnaJ heat shock protein family (Hsp40) member C3 (DNAJC3)
219067_s_at	1.9095	0.0146	NSMCE4A	NSE4 homolog A, SMC5-SMC6 complex component (NSMCE4A)
52731_at	-1.4557	0.0146	AMBRA1	autophagy and beclin 1 regulator 1 (AMBRA1)
1561615_s_at	2.3000	0.0146	SLC8A1	solute carrier family 8 member A1 (SLC8A1)
208010_s_at	-1.5750	0.0147	PTPN22	protein tyrosine phosphatase, non-receptor type 22 (PTPN22)
222807_at	1.2302	0.0147	EMSY	EMSY, BRCA2 interacting transcriptional repressor (EMSY)
200934_at	1.4911	0.0148	DEK	DEK proto-oncogene (DEK)
230006_s_at	2.6796	0.0148	SVIP	small VCP interacting protein (SVIP)
204023_at	1.7144	0.0150	RFC4	replication factor C subunit 4 (RFC4)
223493_at	1.8467	0.0152	FBXO4	F-box protein 4 (FBXO4)
1553906_s_at	1.2276	0.0153	FGD2	FYVE, RhoGEF and PH domain containing 2 (FGD2)
209054_s_at	1.3526	0.0153	NSD2	uclear receptor binding SET domain protein 2 (NSD2)
225696_at	1.6972	0.0153	COPS7B	COP9 signalosome subunit 7B (COPS7B)
229331_at	1.9833	0.0155	SPATA18	spermatogenesis associated 18 (SPATA18)
203160_s_at	1.1469	0.0155	RNF8	ring finger protein 8 (RNF8)
39402_at	1.8860	0.0156	IL1B	interleukin 1 beta (IL1B)
202105_at	1.2921	0.0158	IGBP1	immunoglobulin (CD79A) binding protein 1 (IGBP1)
202911_at	1.3034	0.0158	MSH6	mutS homolog 6 (MSH6)

205483_s_at	1.6765	0.0160	ISG15	ISG15 ubiquitin-like modifier (ISG15)
204418_x_at	-1.0380	0.0161	GSTM2	glutathione S-transferase mu 2 (GSTM2)
204418_x_at	-1.0380	0.0161	GSTM1	glutathione S-transferase mu 1 (GSTM1)
202842_s_at	-1.2740	0.0162	DNAJB9	DnaJ heat shock protein family (Hsp40) member B9 (DNAJB9)
202763_at	1.1677	0.0162	CASP3	caspase 3 (CASP3)
220160_s_at	1.0558	0.0163	KPTN	kaptin, actin binding protein (KPTN)
209310_s_at	1.3873	0.0163	CASP4	caspase 4 (CASP4)
225097_at	-1.7557	0.0164	HIPK2	homeodomain interacting protein kinase 2 (HIPK2)
242281_at	2.5947	0.0164	GLUL	glutamate-ammonia ligase (GLUL)
230108_at	2.3364	0.0165	ERCC6	ERCC excision repair 6, chromatin remodeling factor (ERCC6)
203022_at	1.3706	0.0165	RNASEH2A	ribonuclease H2 subunit A (RNASEH2A)
211323_s_at	-2.0472	0.0168	ITPR1	inositol 1,4,5-trisphosphate receptor type 1 (ITPR1)
201746_at	1.7735	0.0169	TP53	tumor protein p53 (TP53)
221931_s_at	1.0832	0.0170	SEH1L	SEH1 like nucleoporin (SEH1L)
204622_x_at	3.4868	0.0170	NR4A2	nuclear receptor subfamily 4 group A member 2 (NR4A2)
226048_at	1.1930	0.0170	MAPK8	mitogen-activated protein kinase 8 (MAPK8)
1558938_at	3.0766	0.0171	PSME1	proteasome activator subunit 1 (PSME1)
224591_at	1.0505	0.0173	HP1BP3	heterochromatin protein 1 binding protein 3 (HP1BP3)
203171_s_at	1.0212	0.0176	RRP8	ribosomal RNA processing 8, methyltransferase, homolog (yeast) (RRP8)
205672_at	1.3707	0.0176	XPA	XPA, DNA damage recognition and repair factor (XPA)
202431_s_at	1.1770	0.0176	MYC	v-myc avian myelocytomatosis viral oncogene homolog (MYC)
202073_at	1.1093	0.0177	OPTN	Optineurin (OPTN)
219215_s_at	1.6048	0.0177	SLC39A4	solute carrier family 39 member 4 (SLC39A4)
203526_s_at	-1.8957	0.0179	APC	APC, WNT signaling pathway regulator (APC)
33322_i_at	-1.3740	0.0179	SFN	Stratifin (SFN)
235754_at	-2.2089	0.0179	HFE	Hemochromatosis (HFE)
201053_s_at	1.1670	0.0181	PSMF1	proteasome inhibitor subunit 1 (PSMF1)
209349_at	-1.5863	0.0182	RAD50	RAD50 double strand break repair

				protein (RAD50)
1552329_at	2.6277	0.0183	RBBP6	RB binding protein 6, ubiquitin ligase (RBBP6)
203315_at	1.1304	0.0185	NCK2	NCK adaptor protein 2 (NCK2)
1560017_at	-1.0583	0.0185	TMTC3	transmembrane and tetratricopeptide repeat containing 3 (TMTC3)
208436_s_at	1.7210	0.0189	IRF7	interferon regulatory factor 7 (IRF7)
204748_at	1.9749	0.0191	PTGS2	prostaglandin-endoperoxide synthase 2 (PTGS2)
241425_at	-2.7343	0.0191	NUP58	nucleoporin 58(NUP58)
216241_s_at	1.2579	0.0193	TCEA1	transcription elongation factor A1 (TCEA1)
223159_s_at	1.1422	0.0193	NEK6	NIMA related kinase 6 (NEK6)
205047_s_at	2.2915	0.0193	ASNS	asparagine synthetase (glutamine-hydrolyzing)(ASNS)
203616_at	1.2997	0.0194	POLB	DNA polymerase beta (POLB)
244428_at	1.8192	0.0195	DNMT3A	DNA methyltransferase 3 alpha (DNMT3A)
222646_s_at	-1.7167	0.0197	ERO1A	endoplasmic reticulum oxidoreductase 1 alpha (ERO1A)
212018_s_at	1.0291	0.0198	RSL1D1	ribosomal L1 domain containing 1 (RSL1D1)
214246_x_at	1.9165	0.0198	MINK1	misshapen like kinase 1 (MINK1)
206976_s_at	-1.1303	0.0199	HSPH1	heat shock protein family H (Hsp110) member 1 (HSPH1)
230300_at	2.8703	0.0202	PSMA5	proteasome subunit alpha 5 (PSMA5)
209824_s_at	1.3400	0.0207	ARNTL	aryl hydrocarbon receptor nuclear translocator like (ARNTL)
219383_at	2.9946	0.0210	PRR5L	proline rich 5 like (PRR5L)
213596_at	2.3761	0.0210	CASP4	caspase 4 (CASP4)
235749_at	-1.8402	0.0210	UGGT2	UDP-glucose glycoprotein glucosyltransferase 2 (UGGT2)
219334_s_at	-1.4848	0.0211	NABP1	nucleic acid binding protein 1(NABP1)
228109_at	1.8172	0.0212	RASGRF2	Ras protein specific guanine nucleotide releasing factor 2 (RASGRF2)
203607_at	1.7497	0.0213	INPP5F	inositol polyphosphate-5-phosphatase F (INPP5F)
223879_s_at	-2.6287	0.0213	OXR1	oxidation resistance 1 (OXR1)
209743_s_at	-1.3636	0.0213	ITCH	itchy E3 ubiquitin protein ligase (ITCH)
202244_at	1.0216	0.0216	PSMB4	proteasome subunit beta 4 (PSMB4)
210480_s_at	-2.2763	0.0216	MYO6	myosin VI (MYO6)

56919_at	1.8901	0.0217	WDR48	WD repeat domain 48 (WDR48)
217736_s_at	1.0525	0.0217	EIF2AK1	eukaryotic translation initiation factor 2 alpha kinase 1 (EIF2AK1)
202062_s_at	-4.7666	0.0217	SEL1L	SEL1L ERAD E3 ligase adaptor subunit (SEL1L)
242300_at	2.2163	0.0218	UBB	ubiquitin B (UBB)
207805_s_at	1.1013	0.0218	PSMD9	proteasome 26S subunit, non-ATPase 9 (PSMD9)
205126_at	1.1141	0.0220	VRK2	vaccinia related kinase 2 (VRK2)
214953_s_at	-2.8294	0.0220	APP	amyloid beta precursor protein (APP)
213734_at	-1.2283	0.0223	RFC5	replication factor C subunit 5 (RFC5)
209418_s_at	-1.1521	0.0225	THOC5	THO complex 5 (THOC5)
219028_at	-1.2784	0.0227	HIPK2	homeodomain interacting protein kinase 2 (HIPK2)
202494_at	1.1265	0.0227	PPIE	peptidylprolyl isomerase E (PPIE)
209615_s_at	1.4380	0.0229	PAK1	p21 (RAC1) activated kinase 1(PAK1)
218346_s_at	1.1288	0.0230	SESN1	sestrin 1 (SESN1)
204672_s_at	-1.1542	0.0232	ANKRD6	ankyrin repeat domain 6 (ANKRD6)
221477_s_at	1.1698	0.0232	SOD2	superoxide dismutase 2, mitochondrial (SOD2)
218689_at	2.2123	0.0235	FANCF	Fanconi anemia complementation group F (FANCF)
203427_at	1.6082	0.0235	ASF1A	anti-silencing function 1A histone chaperone (ASF1A)
203988_s_at	1.7889	0.0235	FUT8	fucosyltransferase 8 (FUT8)
204203_at	1.2073	0.0236	CEBPG	CCAAT/enhancer binding protein gamma (CEBPG)
225115_at	-1.7948	0.0238	HIPK2	homeodomain interacting protein kinase 2 (HIPK2)
238813_at	1.5429	0.0238	APEX2	apurinic/apyrimidinic endodeoxyribonuclease 2 (APEX2)
219141_s_at	-1.0916	0.0243	AMBRA1	autophagy and beclin 1 regulator 1 (AMBRA1)
211376_s_at	1.9920	0.0246	NSMCE4A	NSE4 homolog A, SMC5-SMC6 complex component (NSMCE4A)
228506_at	1.9407	0.0247	NSMCE4A	NSE4 homolog A, SMC5-SMC6 complex component (NSMCE4A)
215416_s_at	2.1026	0.0250	STOML2	stomatin like 2 (STOML2)
221841_s_at	1.7739	0.0254	KLF4	Kruppel like factor 4 (KLF4)
228183_s_at	1.1745	0.0254	RPAIN	RPA interacting protein (RPAIN)
229010_at	1.4328	0.0262	CBL	Cbl proto-oncogene (CBL)
201404_x_at	-1.0653	0.0262	PSMB2	proteasome subunit beta 3 (PSMB3)
201391_at	1.1342	0.0264	TRAP1	TNF receptor associated protein 1 (TRAP1)
204961_s_at	3.3847	0.0264	NCF1	neutrophil cytosolic factor 1 (NCF1)

204617_s_at	1.7673	0.0265	ACD	adrenocortical dysplasia homolog (ACD)
225651_at	1.2655	0.0265	UBE2E2	ubiquitin conjugating enzyme E2 E2 (UBE2E2)
222909_s_at	1.3891	0.0266	BAG4	BCL2 associated athanogene 4 (BAG4)
200602_at	-2.0802	0.0266	APP	amyloid beta precursor protein (APP)
210257_x_at	-1.1531	0.0267	CUL4B	cullin 4B (CUL4B)
218671_s_at	1.1264	0.0268	ATPIF1	ATPase inhibitory factor 1 (ATPIF1)
221253_s_at	-1.1705	0.0271	TXNDC5	thioredoxin domain containing 5 (TXNDC5)
210354_at	3.4520	0.0271	IFNG	interferon gamma (IFNG)
201222_s_at	-1.4846	0.0273	RAD23B	RAD23 homolog B, nucleotide excision repair protein (RAD23B)
211832_s_at	-1.7581	0.0273	MDM2	MDM2 proto-oncogene (MDM2)
212331_at	1.0703	0.0274	RBL2	RB transcriptional corepressor like 2 (RBL2)
218878_s_at	1.5020	0.0275	SIRT1	sirtuin 1 (SIRT1)
213170_at	2.3971	0.0275	GPX7	glutathione peroxidase 7 (GPX7)
218340_s_at	-1.7507	0.0275	UBA6	ubiquitin like modifier activating enzyme 6 (UBA6)
240413_at	2.2689	0.0277	PYHIN1	pyrin and HIN domain family member 1 (PYHIN1)
201631_s_at	1.3549	0.0281	IER3	immediate early response 3 (IER3)
227628_at	-1.1972	0.0283	GPX8	glutathione peroxidase 8 (putative) (GPX8)
203527_s_at	-1.5834	0.0284	APC	APC, WNT signaling pathway regulator (APC)
212252_at	1.0645	0.0284	CAMKK2	calcium/calmodulin dependent protein kinase kinase 2 (CAMKK2)
225470_at	2.4713	0.0288	NUP35	nucleoporin 35 (NUP35)
233019_at	1.1693	0.0288	CNOT7	CCR4-NOT transcription complex subunit 7 (CNOT7)
203588_s_at	1.5842	0.0289	TFDP2	transcription factor Dp-2 (TFDP2)
203103_s_at	1.3563	0.0291	PRPF19	pre-mRNA processing factor 19 (PRPF19)
227119_at	1.2457	0.0292	CNOT6L	CCR4-NOT transcription complex subunit 6 like (CNOT6L)
218463_s_at	1.0056	0.0294	MUS81	MUS81 structure-specific endonuclease subunit (MUS81)
200889_s_at	-1.2155	0.0300	SSR1	signal sequence receptor subunit 1 (SSR1)
214843_s_at	-1.1260	0.0304	USP33	ubiquitin specific peptidase 33 (USP33)
226008_at	1.1566	0.0307	NSMCE3	NSE3 homolog, SMC5-SMC6 complex component (NSMCE3)

1553096_s_at	1.1773	0.0309	BCL2L11	BCL2 like 11 (BCL2L11)
200880_at	1.0309	0.0309	DNAJA1	DnaJ heat shock protein family (Hsp40) member A1 (DNAJA1)
232206_at	-1.8102	0.0309	ULK4	unc-51 like kinase 4 (ULK4)
1554251_at	1.8315	0.0311	HP1BP3	heterochromatin protein 1 binding protein 3(HP1BP3)
219578_s_at	-3.2788	0.0311	CPEB1	cytoplasmic polyadenylation element binding protein 1 (CPEB1)
229141_at	1.9646	0.0312	WDR33	WD repeat domain 33 (WDR33)
207727_s_at	1.0357	0.0312	MUTYH	mutY DNA glycosylase (MUTYH)
227143_s_at	1.1127	0.0312	BID	BH3 interacting domain death agonist (BID)
225923_at	1.4085	0.0313	VAPB	VAMP associated protein B and C (VAPB)
31874_at	1.0400	0.0314	GAS2L1	growth arrest specific 2 like 1(GAS2L1)
203577_at	1.1988	0.0319	GTF2H4	general transcription factor IIH subunit 4 (GTF2H4)
203358_s_at	3.1157	0.0320	EZH2	enhancer of zeste 2 polycomb repressive complex 2 subunit (EZH2)
212749_s_at	1.4305	0.0321	RCHY1	ring finger and CHY zinc finger domain containing 1 (RCHY1)
239810_at	1.2337	0.0322	VASH1	vasohibin 1 (VASH1)
203805_s_at	1.2728	0.0323	FANCA	Fanconi anemia complementation group A (FANCA)
202843_at	-1.5760	0.0325	DNAJB9	DnaJ heat shock protein family (Hsp40) member B9 (DNAJB9)
204832_s_at	-1.5563	0.0332	BMPR1A	bone morphogenetic protein receptor type 1A (BMPR1A)
225116_at	-2.4597	0.0332	HIPK2	homeodomain interacting protein kinase 2 (HIPK2)
234362_s_at	2.4117	0.0333	CTLA4	cytotoxic T-lymphocyte associated protein 4 (CTLA4)
222343_at	1.1843	0.0334	BCL2L11	BCL2 like 11 (BCL2L11)
227027_at	-1.0695	0.0337	GFPT1	glutamine--fructose-6-phosphate transaminase 1 (GFPT1)
205081_at	2.3734	0.0340	CRIP1	cysteine rich protein 1 (CRIP1)
202638_s_at	1.7367	0.0343	ICAM1	intercellular adhesion molecule 1 (ICAM1)
201211_s_at	-1.0638	0.0345	DDX3X	DEAD-box helicase 3, X-linked (DDX3X)
235850_at	1.5725	0.0351	FAM162A	family with sequence similarity 162 member A (FAM162A)
202625_at	1.3497	0.0352	LYN	LYN proto-oncogene, Src family tyrosine kinase (LYN)
202401_s_at	1.0717	0.0355	SRF	serum response factor(SRF)

200758_s_at	-1.2326	0.0357	NFE2L1	nuclear factor, erythroid 2 like 1 (NFE2L1)
203817_at	1.9985	0.0358	GUCY1B3	guanylate cyclase 1 soluble subunit beta (GUCY1B3)
235341_at	-2.9540	0.0359	DNAJC3	DnaJ heat shock protein family (Hsp40) member C3 (DNAJC3)
217735_s_at	1.3169	0.0359	EIF2AK1	eukaryotic translation initiation factor 2 alpha kinase 1 (EIF2AK1)
213007_at	1.1502	0.0360	FANCI	Fanconi anemia complementation group I (FANCI)
213750_at	1.7795	0.0367	RSL1D1	ribosomal L1 domain containing 1 (RSL1D1)
202412_s_at	1.9167	0.0368	USP1	ubiquitin specific peptidase 1 (USP1)
206665_s_at	-1.8977	0.0369	BCL2L1	BCL2 like 1 (BCL2L1)
201316_at	1.6425	0.0370	PSMA2	proteasome subunit alpha 2 (PSMA2)
223275_at	2.4144	0.0375	PRMT6	protein arginine methyltransferase 6 (PRMT6)
205067_at	2.1878	0.0380	IL1B	interleukin 1 beta (IL1B)
207039_at	2.2441	0.0380	CDKN2A	cyclin dependent kinase inhibitor 2A (CDKN2A)
225824_at	1.3895	0.0382	CCNK	cyclin K (CCNK)
217127_at	-1.7073	0.0385	CTH	cystathionine gamma-lyase (CTH)
211595_s_at	1.0919	0.0386	MRPS11	mitochondrial ribosomal protein S11 (MRPS11)
224792_at	-2.2003	0.0389	TNKS1BP1	tankyrase 1 binding protein 1 (TNKS1BP1)
221830_at	-2.3497	0.0392	RAP2A	RAP2A, member of RAS oncogene family (RAP2A)
229720_at	1.1039	0.0392	BAG1	BCL2 associated athanogene 1 (BAG1)
223960_s_at	1.0203	0.0394	CDIP1	cell death inducing p53 target 1 (CDIP1)
212751_at	1.1923	0.0395	UBE2N	ubiquitin conjugating enzyme E2 N (UBE2N)
209456_s_at	-2.3494	0.0396	FBXW11	F-box and WD repeat domain containing 11 (FBXW11)
208692_at	1.4602	0.0397	RPS3	ribosomal protein S3 (RPS3)
207108_s_at	-1.9856	0.0398	NIPBL	NIPBL, cohesin loading factor (NIPBL)
215533_s_at	-1.9690	0.0399	UBE4B	ubiquitination factor E4B (UBE4B)
201002_s_at	1.2194	0.0400	UBE2V1	ubiquitin conjugating enzyme E2 V1 (UBE2V1)
205909_at	2.1843	0.0408	POLE2	DNA polymerase epsilon 2, accessory subunit (POLE2)
220066_at	1.9755	0.0408	NOD2	nucleotide binding oligomerization domain containing 2 (NOD2)
209511_at	1.1086	0.0408	POLR2F	RNA polymerase II subunit F

				(POLR2F)
221331_x_at	1.8292	0.0409	CTLA4	cytotoxic T-lymphocyte associated protein 4 (CTLA4)
203216_s_at	-1.1468	0.0410	MYO6	myosin VI (MYO6)
223339_at	2.3401	0.0412	ATPIF1	ATPase inhibitory factor 1 (ATPIF1)
38290_at	1.0282	0.0419	RGS14	regulator of G-protein signaling 14 (RGS14)
225836_s_at	1.8093	0.0420	RHNO1	RAD9-HUS1-RAD1 interacting nuclear orphan 1 (RHNO1)
204131_s_at	-2.0174	0.0421	FOXO3	forkhead box O3 (FOXO3)
205811_at	1.3020	0.0424	POLG2	DNA polymerase gamma 2, accessory subunit (POLG2)
227678_at	1.1093	0.0424	ATP23	ATP23 metallopeptidase and ATP synthase assembly factor homolog (ATP23)
213136_at	1.2147	0.0425	PTPN2	protein tyrosine phosphatase, non-receptor type 2 (PTPN2)
225589_at	-1.0881	0.0429	SH3RF1	SH3 domain containing ring finger 1 (SH3RF1)
232287_at	2.7107	0.0429	ERCC6	ERCC excision repair 6, chromatin remodeling factor (ERCC6)
211506_s_at	-4.1043	0.0432	CXCL8	C-X-C motif chemokine ligand 8 (CXCL8)
202466_at	1.1560	0.0433	PAPD7	poly(A) RNA polymerase D7, non-canonical (PAPD7)
218499_at	1.6223	0.0434	STK26	serine/threonine protein kinase 26 (STK26)
211863_x_at	-1.0014	0.0434	HFE	Hemochromatosis (HFE)
230192_at	1.2646	0.0436	TRIM13	tripartite motif containing 13 (TRIM13)
204621_s_at	2.0158	0.0436	NR4A2	nuclear receptor subfamily 4 group A member 2 (NR4A2)
208948_s_at	1.1438	0.0438	STAU1	staufen double-stranded RNA binding protein 1 (STAU1)
226022_at	-1.1266	0.0438	SASH1	SAM and SH3 domain containing 1 (SASH1)
204824_at	1.0160	0.0438	ENDOG	endonuclease G (ENDOG)
235609_at	2.3943	0.0443	BRIP1	BRCA1 interacting protein C-terminal helicase 1 (BRIP1)
225144_at	-1.0022	0.0443	BMPR2	bone morphogenetic protein receptor type 2 (BMPR2)
212927_at	1.2228	0.0450	SMC5	structural maintenance of chromosomes 5 (SMC5)
220342_x_at	-1.7405	0.0463	EDEM3	ER degradation enhancing alpha-mannosidase like protein 3 (EDEM3)
1554411_at	-4.2264	0.0466	CTNNB1	catenin beta 1(CTNNB1)

209994_s_at	-1.0281	0.0468	ABCB4	ATP binding cassette subfamily B member 4 (ABCB4)
243000_at	1.8848	0.0469	CDK6	cyclin dependent kinase 6 (CDK6)
226939_at	-1.0229	0.0474	CPEB2	cytoplasmic polyadenylation element binding protein 2 (CPEB2)
231873_at	-1.1004	0.0479	BMPR2	bone morphogenetic protein receptor type 2 (BMPR2)
228925_at	1.4197	0.0480	MAPKAPK 5	mitogen-activated protein kinase-activated protein kinase 5 (MAPKAPK5)
213357_at	1.1921	0.0480	GTF2H5	general transcription factor IIH subunit 5 (GTF2H5)
201502_s_at	1.4184	0.0480	NFKBIA	NFKB inhibitor alpha (NFKBIA)
218608_at	-4.2617	0.0480	ATP13A2	ATPase 13A2 (ATP13A2)
201115_at	1.1993	0.0485	POLD2	DNA polymerase delta 2, accessory subunit (POLD2)
200764_s_at	-1.0486	0.0485	CTNNA1	catenin alpha 1 (CTNNA1)
202859_x_at	-1.6208	0.0486	CXCL8	C-X-C motif chemokine ligand 8 (CXCL8)

COPD				
Affy probe ID	**logFC**	**q value**	**Name**	**Gene name**
213931_at	-1.6783	0.0002	ID2	inhibitor of DNA binding 2, HLH protein (ID2)
203234_at	1.3446	0.0148	UPP1	uridine phosphorylase 1 (UPP1)
227073_at	-1.1097	0.0155	MAP3K2	mitogen-activated protein kinase kinase kinase 2 (MAP3K2)
200632_s_at	1.4802	0.0162	NDRG1	N-myc downstream regulated 1 (NDRG1)
225207_at	-1.7186	0.0162	PDK4	pyruvate dehydrogenase kinase 4 (PDK4)
236539_at	-1.0176	0.0200	PTPN22	protein tyrosine phosphatase, non-receptor type 22 (PTPN22)
203379_at	1.0091	0.0200	RPS6KA1	ribosomal protein S6 kinase A1 (RPS6KA1)
242669_at	-1.2042	0.0222	UFM1	ubiquitin fold modifier 1 (UFM1)
214048_at	-1.0364	0.0247	MBD4	methyl-CpG binding domain 4, DNA glycosylase (MBD4)
221768_at	-1.4014	0.0254	SFPQ	splicing factor proline and glutamine rich (SFPQ)
242300_at	1.3782	0.0292	UBB	ubiquitin B (UBB)
200895_s_at	1.0642	0.0296	FKBP4	FK506 binding protein 4 (FKBP4)

203315_at	1.9792	0.0319	NCK2	NCK adaptor protein 2 (NCK2)
241752_at	-1.0278	0.0319	SLC8A1	solute carrier family 8 member A1 (SLC8A1)
201565_s_at	-1.1118	0.0328	ID2	inhibitor of DNA binding 2, HLH protein (ID2)
202393_s_at	-1.0453	0.0329	KLF10	Kruppel like factor 10 (KLF10)
215037_s_at	1.5925	0.0330	BCL2L1	BCL2 like 1 (BCL2L1)
229221_at	-1.0147	0.0333	CD44	CD44 molecule (Indian blood group) (CD44)
228506_at	-1.2858	0.0341	NSMCE4A	NSE4 homolog A, SMC5-SMC6 complex component (NSMCE4A)
202073_at	1.1746	0.0360	OPTN	Optineurin (OPTN)
202539_s_at	-2.1819	0.0362	HMGCR	3-hydroxy-3-methylglutaryl-CoA reductase (HMGCR)
201848_s_at	1.8162	0.0366	BNIP3	BCL2 interacting protein 3 (BNIP3)
218801_at	-1.0358	0.0369	UGGT2	UDP-glucose glycoprotein glucosyltransferase 2 (UGGT2)
243751_at	-1.1260	0.0399	CHD2	chromodomain helicase DNA binding protein 2 (CHD2)
1556583_a_at	-1.1444	0.0399	SLC8A1	solute carrier family 8 member A1 (SLC8A1)
201626_at	-1.5651	0.0423	INSIG1	insulin induced gene 1 (INSIG1)
207540_s_at	1.0715	0.0459	SYK	spleen associated tyrosine kinase (SYK)

Table E4 Differentially regulated gene probes belonging to GO term Oxidative Stress

Healthy				
Affy probe ID	**logFC**	**q value**	**Name**	**Gene Name**
204639_at	2.4216	0.0136	ADA	adenosine deaminase(ADA)
202381_at	-1.1223	0.0147	ADAM9	ADAM metallopeptidase domain 9 (ADAM9)
203322_at	1.4707	0.0095	ADNP2	ADNP homeobox 2(ADNP2)
209901_x_at	2.1444	0.0055	AIF1	allograft inflammatory factor 1 (AIF1)
213095_x_at	2.0801	0.0046	AIF1	allograft inflammatory factor 1 (AIF1)
215051_x_at	1.8362	0.0058	AIF1	allograft inflammatory factor 1 (AIF1)
201272_at	-1.4230	0.0039	AKR1B1	aldo-keto reductase family 1 member B (AKR1B1)
226291_at	-1.1426	0.0069	ALS2	ALS2, alsin Rho guanine nucleotide exchange factor (ALS2)
200602_at	-2.0802	0.0266	APP	amyloid beta precursor protein (APP)
214953_s_at	-2.8294	0.0220	APP	amyloid beta precursor protein (APP)
209824_s_at	1.3400	0.0207	ARNTL	aryl hydrocarbon receptor nuclear translocator like (ARNTL)
203454_s_at	1.5541	0.0018	ATOX1	antioxidant 1 copper chaperone (ATOX1)
218608_at	-4.2617	0.0480	ATP13A2	ATPase 13A2(ATP13A2)
205197_s_at	-4.3706	0.0016	ATP7A	ATPase copper transporting alpha (ATP7A)
212517_at	-1.3649	0.0348	ATRN	Attractin (ATRN)
212252_at	1.0645	0.0284	CAMKK2	calcium/calmodulin dependent protein kinase kinase 2 (CAMKK2)
202763_at	1.1677	0.0162	CASP3	caspase 3 (CASP3)
203418_at	3.2141	0.0029	CCNA2	cyclin A2 (CCNA2)
213226_at	2.8150	0.0045	CCNA2	cyclin A2 (CCNA2)
206488_s_at	-2.1956	0.0014	CD36	CD36 molecule (CD36)
209555_s_at	-2.4553	0.0015	CD36	CD36 molecule (CD36)
228766_at	-2.2228	0.0036	CD36	CD36 molecule (CD36)
242197_x_at	-1.6963	0.0104	CD36	CD36 molecule (CD36)
205692_s_at	3.4131	0.0006	CD38	CD38 molecule (CD38)
203213_at	4.7116	0.0059	CDK1	cyclin dependent kinase 1 (CDK1)
203214_x_at	3.8980	0.0032	CDK1	cyclin dependent kinase 1 (CDK1)
226939_at	-1.0229	0.0474	CPEB2	cytoplasmic polyadenylation element binding protein 2 (CPEB2)
1554411_at	-4.2264	0.0466	CTNNB1	catenin beta 1(CTNNB1)
226632_at	-1.5163	0.0099	CYGB	Cytoglobin (CYGB)
204824_at	1.0160	0.0438	ENDOG	endonuclease G (ENDOG)
200878_at	-1.6743	0.0009	EPAS1	endothelial PAS domain protein 1

				(EPAS1)
200879_s_at	-3.4515	0.0025	EPAS1	endothelial PAS domain protein 1 (EPAS1)
203719_at	1.3789	0.0094	ERCC1	ERCC excision repair 1, endonuclease non-catalytic subunit (ERCC1)
207347_at	2.6408	0.0035	ERCC6	ERCC excision repair 6, chromatin remodeling factor (ERCC6)
230108_at	2.3364	0.0165	ERCC6	ERCC excision repair 6, chromatin remodeling factor (ERCC6)
232287_at	2.7107	0.0429	ERCC6	ERCC excision repair 6, chromatin remodeling factor (ERCC6)
218498_s_at	-1.4255	0.0142	ERO1A	endoplasmic reticulum oxidoreductase 1 alpha (ERO1A)
222646_s_at	-1.7167	0.0197	ERO1A	endoplasmic reticulum oxidoreductase 1 alpha (ERO1A)
224833_at	4.4827	0.0015	ETS1	ETS proto-oncogene 1, transcription factor (ETS1)
203358_s_at	3.1157	0.0320	EZH2	enhancer of zeste 2 polycomb repressive complex 2 subunit (EZH2)
232064_at	-1.1974	0.0050	FER	FER tyrosine kinase (FER)
202724_s_at	1.5573	0.0055	FOXO1	forkhead box O1 (FOXO1)
204131_s_at	-2.0174	0.0421	FOXO3	forkhead box O3 (FOXO3)
203988_s_at	1.7889	0.0235	FUT8	fucosyltransferase 8 (FUT8)
204224_s_at	5.3079	0.0008	GCH1	GTP cyclohydrolase 1 (GCH1)
202922_at	1.2872	0.0040	GCLC	glutamate-cysteine ligase catalytic subunit (GCLC)
202923_s_at	1.2349	0.0027	GCLC	glutamate-cysteine ligase catalytic subunit (GCLC)
223278_at	3.0753	0.0030	GJB2	gap junction protein beta 2 (GJB2)
213170_at	2.3971	0.0275	GPX7	glutathione peroxidase 7 (GPX7)
227628_at	-1.1972	0.0283	GPX8	glutathione peroxidase 8 (putative) (GPX8)
203817_at	1.9985	0.0358	GUCY1B3	guanylate cyclase 1 soluble subunit beta (GUCY1B3)
206976_s_at	-1.1303	0.0199	HSPH1	heat shock protein family H (Hsp110) member 1 (HSPH1)
208744_x_at	-1.5729	0.0134	HSPH1	heat shock protein family H (Hsp110) member 1 (HSPH1)
207072_at	3.6333	0.0020	IL18RAP	interleukin 18 receptor accessory protein (IL18RAP)
221841_s_at	1.7739	0.0254	KLF4	Kruppel like factor 4 (KLF4)
209653_at	-1.0706	0.0064	KPNA4	karyopherin subunit alpha 4 (KPNA4)
1552263_at	2.1817	0.0057	MAPK1	mitogen-activated protein kinase 1 (MAPK1)
226048_at	1.1930	0.0170	MAPK8	mitogen-activated protein kinase 8

				(MAPK8)
200797_s_at	1.4190	0.0029	MCL1	BCL2 family apoptosis regulator (MCL1)
200798_x_at	1.4244	0.0055	MCL1	BCL2 family apoptosis regulator (MCL1)
205386_s_at	-1.6688	0.0128	MDM2	MDM2 proto-oncogene (MDM2)
211832_s_at	-1.7581	0.0273	MDM2	MDM2 proto-oncogene (MDM2)
217373_x_at	-1.5002	0.0018	MDM2	MDM2 proto-oncogene (MDM2)
225160_x_at	-3.3167	0.0041	MDM2	MDM2 proto-oncogene (MDM2)
203510_at	-4.5338	0.0016	MET	MET proto-oncogene, receptor tyrosine kinase (MET)
1565162_s_at	-1.5077	0.0065	MGST1	microsomal glutathione S-transferase 1 (MGST1)
224918_x_at	-1.0379	0.0042	MGST1	microsomal glutathione S-transferase 1 (MGST1)
231736_x_at	-1.0800	0.0033	MGST1	microsomal glutathione S-transferase 1 (MGST1)
205905_s_at	-2.3166	0.0022	MICB	MHC class I polypeptide-related sequence B (MICB)
228528_at	1.4066	0.0059	MIR29B2	microRNA 29b-2 (MIR29B2)
204798_at	4.2929	0.0052	MYB	MYB proto-oncogene, transcription factor (MYB)
204961_s_at	3.3847	0.0264	NCF1	neutrophil cytosolic factor 1 (NCF1)
214084_x_at	2.9014	0.0054	NCF1	neutrophil cytosolic factor 1 (NCF1)
225344_at	1.3596	0.0068	NCOA7	nuclear receptor coactivator 7 (NCOA7)
223244_s_at	1.4173	0.0086	NDUFA12	NADH:ubiquinone oxidoreductase subunit A12 (NDUFA12)
203190_at	1.1449	0.0072	NDUFS8	NADH:ubiquinone oxidoreductase core subunit S8 (NDUFS8)
201829_at	2.3673	0.0053	NET1	neuroepithelial cell transforming 1 (NET1)
201830_s_at	3.1156	0.0029	NET1	neuroepithelial cell transforming 1 (NET1)
200758_s_at	-1.2326	0.0357	NFE2L1	nuclear factor, erythroid 2 like 1 (NFE2L1)
220384_at	3.4506	0.0016	NME8	NME/NM23 family member 8 (NME8)
204621_s_at	2.0158	0.0436	NR4A2	nuclear receptor subfamily 4 group A member 2 (NR4A2)
204622_x_at	3.4868	0.0170	NR4A2	nuclear receptor subfamily 4 group A member 2 (NR4A2)
216248_s_at	3.3321	0.0142	NR4A2	nuclear receptor subfamily 4 group A member 2 (NR4A2)
209959_at	6.1518	0.0014	NR4A3	nuclear receptor subfamily 4 group A member 3 (NR4A3)

218609_s_at	1.9037	0.0048	NUDT2	nudix hydrolase 2 (NUDT2)
218197_s_at	-1.8142	0.0018	OXR1	oxidation resistance 1 (OXR1)
223879_s_at	-2.6287	0.0213	OXR1	oxidation resistance 1 (OXR1)
201202_at	2.0012	0.0054	PCNA	proliferating cell nuclear antigen (PCNA)
206686_at	-1.6488	0.0086	PDK1	pyruvate dehydrogenase kinase 1 (PDK1)
201489_at	1.2158	0.0081	PPIF	peptidylprolyl isomerase F (PPIF)
242751_at	-1.6397	0.0103	PRDX6	peroxiredoxin 6 (PRDX6)
209139_s_at	1.3821	0.0102	PRKRA	protein activator of interferon induced protein kinase EIF2AK2 (PRKRA)
219383_at	2.9946	0.0210	PRR5L	proline rich 5 like (PRR5L)
203460_s_at	-1.0503	0.0031	PSEN1	presenilin 1 (PSEN1)
205961_s_at	4.2381	0.0034	PSIP1	PC4 and SFRS1 interacting protein 1 (PSIP1)
209337_at	4.3718	0.0027	PSIP1	PC4 and SFRS1 interacting protein 1 (PSIP1)
204748_at	1.9749	0.0191	PTGS2	prostaglandin-endoperoxide synthase 2 (PTGS2)
200651_at	1.3886	0.0082	RACK1	receptor for activated C kinase 1 (RACK1)
38290_at	1.0282	0.0419	RGS14	regulator of G-protein signaling 14 (RGS14)
212099_at	2.9696	0.0087	RHOB	ras homolog family member B (RHOB)
224972_at	1.3415	0.0137	ROMO1	reactive oxygen species modulator 1 (ROMO1)
208692_at	1.4602	0.0397	RPS3	ribosomal protein S3 (RPS3)
201286_at	-1.4633	0.0052	SDC1	syndecan 1 (SDC1)
201287_s_at	-2.5360	0.0010	SDC1	sestrin 1 (SESN1)
218346_s_at	1.1288	0.0230	SESN1	sestrin 3(SESN3)
225123_at	2.7206	0.0093	SESN3	SIN3 transcription regulator family member A (SIN3A)
225135_at	2.7524	0.0046	SIN3A	SIN3 transcription regulator family member A (SIN3A)
238005_s_at	1.9612	0.0047	SIN3A	SIN3 transcription regulator family member A (SIN3A)
218878_s_at	1.5020	0.0275	SIRT1	sirtuin 1 (SIRT1)
211572_s_at	-2.1236	0.0015	SLC23A2	solute carrier family 23 member 2 (SLC23A2)
209921_at	3.3825	0.0026	SLC7A11	solute carrier family 7 member 11 (SLC7A11)
217678_at	4.4084	0.0092	SLC7A11	solute carrier family 7 member 11 (SLC7A11)

1561615_s_at	2.3000	0.0146	SLC8A1	solute carrier family 8 member A1 (SLC8A1)
204466_s_at	-5.0755	0.0011	SNCA	synuclein alpha (SNCA)
204467_s_at	-2.2398	0.0041	SNCA	synuclein alpha (SNCA)
207827_x_at	-4.1027	0.0030	SNCA	synuclein alpha (SNCA)
211546_x_at	-3.0292	0.0041	SNCA	synuclein alpha(SNCA)
200642_at	1.1138	0.0033	SOD1	superoxide dismutase 1, soluble (SOD1)
215223_s_at	2.2428	0.0019	SOD2	superoxide dismutase 2, mitochondrial (SOD2)
221477_s_at	1.1698	0.0232	SOD2	superoxide dismutase 2, mitochondria l(SOD2)
225252_at	1.0819	0.0056	SRXN1	sulfiredoxin 1 (SRXN1)
208948_s_at	1.1438	0.0438	STAU1	staufen double-stranded RNA binding protein 1 (STAU1)
218499_at	1.6223	0.0434	STK26	serine/threonine protein kinase 26 (STK26)
1552798_a_at	-1.8891	0.0065	TLR4	toll like receptor 4 (TLR4)
207113_s_at	3.9122	0.0017	TNF	tumor necrosis factor (TNF)
202644_s_at	2.7125	0.0015	TNFAIP3	TNF alpha induced protein 3 (TNFAIP3)
201746_at	1.7735	0.0169	TP53	tumor protein p53 (TP53)
201391_at	1.1342	0.0264	TRAP1	TNF receptor associated protein 1(TRAP1)
221906_at	2.9456	0.0206	TXNRD3	thioredoxin reductase 3 (TXNRD3)
59631_at	2.5450	0.0064	TXNRD3	thioredoxin reductase 3 (TXNRD3)
1558549_s_at	-4.5040	0.0015	VNN1	vanin 1 (VNN1)
205844_at	-3.9550	0.0063	VNN1	vanin 1 (VNN1)
205126_at	1.1141	0.0220	VRK2	vaccinia related kinase 2 (VRK2)
205672_at	1.3707	0.0176	XPA	XPA, DNA damage recognition and repair facto r(XPA)

COPD				
Affy probe ID	**logFC**	**q value**	**Name**	**Gene Name**
1556583_a_at	-1.1444	0.0399	SLC8A1	solute carrier family 8 member A1 (SLC8A1)
201848_s_at	1.8162	0.0366	BNIP3	BCL2 interacting protein 3 (BNIP3)
221768_at	-1.4014	0.0254	SFPQ	splicing factor proline and glutamine rich (SFPQ)
241752_at	-1.0278	0.0319	SLC8A1	solute carrier family 8 member A1 (SLC8A1)

Table E5 Nrf2 gene probes differentially regulated by infection in healthy AM

Healthy				
Affy probe ID	**logFC**	**q value**	**Name**	**Gene name**
205890_s_at	7.4702	0.0006	GABBR1	gamma-aminobutyric acid type B receptor subunit 1(GABBR1)
202922_at	1.2872	0.0040	GCLC	glutamate-cysteine ligase catalytic subunit(GCLC)
202923_s_at	1.2349	0.0027	GCLC	glutamate-cysteine ligase catalytic subunit(GCLC)
213170_at	2.3971	0.0275	GPX7	glutathione peroxidase 7(GPX7)
201415_at	0.8484	0.0322	GSS	glutathione synthetase(GSS)
209531_at	1.5210	0.0255	GSTZ1	glutathione S-transferase zeta 1(GSTZ1)
201468_s_at	0.7719	0.0249	NQO1	NAD(P)H quinone dehydrogenase 1(NQO1)
217678_at	4.4084	0.0092	SLC7A11	solute carrier family 7 member 11(SLC7A11)
209921_at	3.3825	0.0026	SLC7A11	solute carrier family 7 member 11(SLC7A11)
200642_at	1.1138	0.0033	SOD1	superoxide dismutase 1, soluble(SOD1)
209077_at	0.8171	0.0303	TXN2	thioredoxin 2(TXN2)

COPD				
Affy probe ID	**logFC**	**q value**	**Name**	**Gene name**
209213_at	0.7155	0.0626	CBR1	carbonyl reductase 1 (CBR1)
205890_s_at	0.0068	0.6882	GABBR1	gamma-aminobutyric acid type B receptor subunit 1 (GABBR1)
1555330_at	-0.6511	0.2319	GCLC	glutamate-cysteine ligase catalytic subunit (GCLC)
213170_at	-0.0063	0.6882	GPX7	glutathione peroxidase 7 (GPX7)
211630_s_at	0.2954	0.1261	GSS	glutathione synthetase (GSS)
209531_at	-0.1778	0.4997	GSTZ1	glutathione S-transferase zeta 1 (GSTZ1)
210519_s_at	0.5614	0.0899	NQO1	NAD(P)H quinone dehydrogenase 1 (NQO1)
207528_s_at	-0.0246	0.6882	SLC7A11	solute carrier family 7 member 11 (SLC7A11)
200642_at	0.1960	0.2304	SOD1	superoxide dismutase 1, soluble (SOD1)
209078_s_at	0.3125	0.1632	TXN2	thioredoxin 2 (TXN2)

Table E6

Demographics for additional non-COPD-MAP patients used in Figure 6 and 7.

	Healthy Non-Smoker	Healthy Smoker	COPD
N	3	1	7
Age (years)	62 (49-69)	55	64(47-72)
Gender	1♀ : 2♂	1♂	3♀ : 4♂
FEV1 Litres	2.69 (1.7-3.29)	3.39	1.89 (1.21-3.77)
FEV1 %	91.98 (86.81-100.33)	94.43	70.8 (48.69-113)
FVC litres	3.56 (2.37-4.49)	4.58	3.3 (1.32-5.28)
GOLD Stage *	N/A	N/A	2 GOLD A 4 GOLD B 0 GOLD C 0 GOLD D
Non-Frequent /Frequent	N/A	N/A	NF 5 (0 Exacerbations = 3, 1 Exacerbation = 2 F 2 (2 Exacerbations =1, 3 Exacerbations =1, >3 Exacerbations =0)
Pack Years	N/A	22.6	36.5 (23.2-55)
Smoking Status: Current/Ex/Never	0/0/3	1/0/0	4/3/0
Inhaled Corticosteroids use	0	0	4
Vaccine	2 Yes, 1 No	N/A	5 Yes, 2 No
St George's Respiratory Questionnaire (SGRQ) Total score *	N/A	N/A	31.97 (4.92-70.28)
COPD Assessment Test (CAT) *	N/A	N/A	16.7 (7-30)
6 Minute Walk (m)	N/A	N/A	N/A

*One patient with assessment not performed

Supplementary References

E1. Hurst JR, Vestbo J, Anzueto A, Locantore N, Mullerova H, Tal-Singer R, Miller B, Lomas DA, Agusti A, Macnee W, Calverley P, Rennard S, Wouters EF, Wedzicha JA, Evaluation of CLtIPSEI. Susceptibility to exacerbation in chronic obstructive pulmonary disease. *N Engl J Med* 2010;363:1128-1138.
E2. Jones PW. St. George's respiratory questionnaire: Mcid. *Copd* 2005;2:75-79.
E3. Jones PW, Harding G, Berry P, Wiklund I, Chen WH, Kline Leidy N. Development and first validation of the copd assessment test. *Eur Respir J* 2009;34:648-654.
E4. Stenton C. The mrc breathlessness scale. *Occup Med (Lond)* 2008;58:226-227.
E5. Ats statement: Guidelines for the six-minute walk test. *Am J Respir Crit Care Med* 2002;166:111-117.
E6. HPA. Uk standards for microbiology investigations investigation of bronchoalveolar lavage, sputum and associated specimens. 2012. Vol B 57:1-36.
E7. Garcha DS, Thurston SJ, Patel AR, Mackay AJ, Goldring JJ, Donaldson GC, McHugh TD, Wedzicha JA. Changes in prevalence and load of airway bacteria using quantitative pcr in stable and exacerbated copd. *Thorax* 2012;67:1075-1080.
E8 Elberse KE, Tcherniaeva I, Berbers GA, Schouls LM. Optimization and application of a multiplex beadbased assay to quantify serotype-specific IgG against Streptococcus pneumoniae polysaccharides: response to the booster vaccine after immunization with the pneumococcal 7-valent conjugate vaccine. *Clinical and vaccine immunology*; 2010: 17:674–82.
E9. Marriott HM, Bingle CD, Read RC, Braley KE, Kroemer G, Hellewell PG, Craig RW, Whyte MK, Dockrell DH. Dynamic changes in mcl-1 expression regulate macrophage viability or commitment to apoptosis during bacterial clearance. *J Clin Invest* 2005;115:359-368.
E10. Gordon SB, Irving GR, Lawson RA, Lee ME, Read RC. Intracellular trafficking and killing of streptococcus pneumoniae by human alveolar macrophages are influenced by opsonins. *Infect Immun* 2000;68:2286-2293.
E11. Dockrell DH, Lee M, Lynch DH, Read RC. Immune-mediated phagocytosis and killing of streptococcus pneumoniae are associated with direct and bystander macrophage apoptosis. *J Infect Dis* 2001;184:713-722.

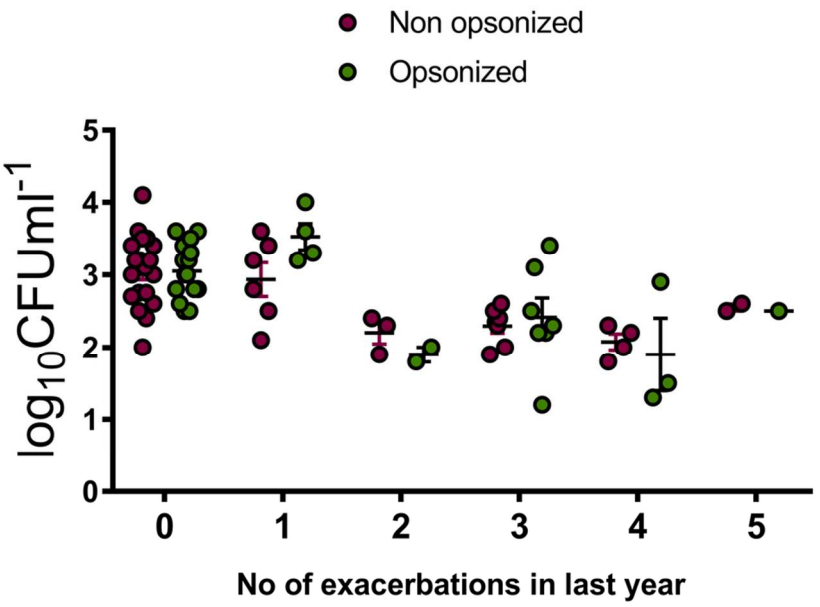

Figure E1. Relationship between bacterial uptake and exacerbation frequency. Alveolar macrophages (AM) were collected from patients with COPD and were challenged with non-opsonized (NO) or opsonized (O) serotype 14 S. pneumoniae for 4 h, before extracellular bacteria were killed by the addition of antibiotics. At the designated time post-antibiotics, viable bacteria in duplicate wells were measured and plotted against exacerbation frequency. 'n' values for NO/O by exacerbation frequency; 0=20/15, 1=7/4, 2=3/2,3=7/74=3/3,5=2/1.

97x68mm (300 x 300 DPI)

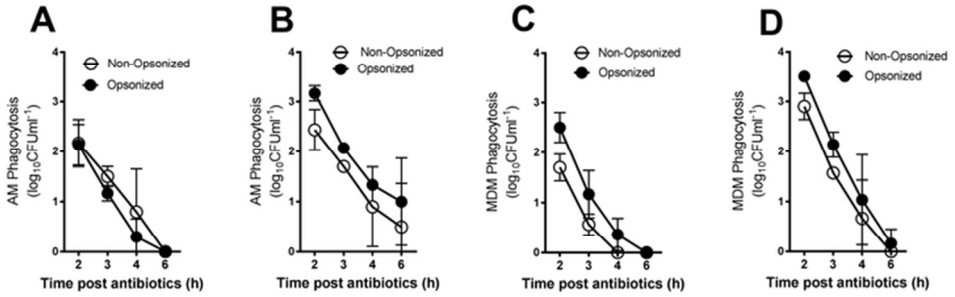

Figure E2. COPD Macrophages show no defect in early-phase bacterial killing. (A-D) Alveolar macrophages (AM) (A and B) or monocyte derived macrophages (MDM) were collected from patients with COPD (A and C) or healthy donors (B and D) and were challenged with non-opsonized or opsonized serotype 14 S. pneumoniae for 4h, before extracellular bacteria were killed by the addition of antibiotics. At the designated time post-antibiotics, viable bacteria in duplicate wells were measured, n=3, no significant differences between any groups.

64x22mm (300 x 300 DPI)

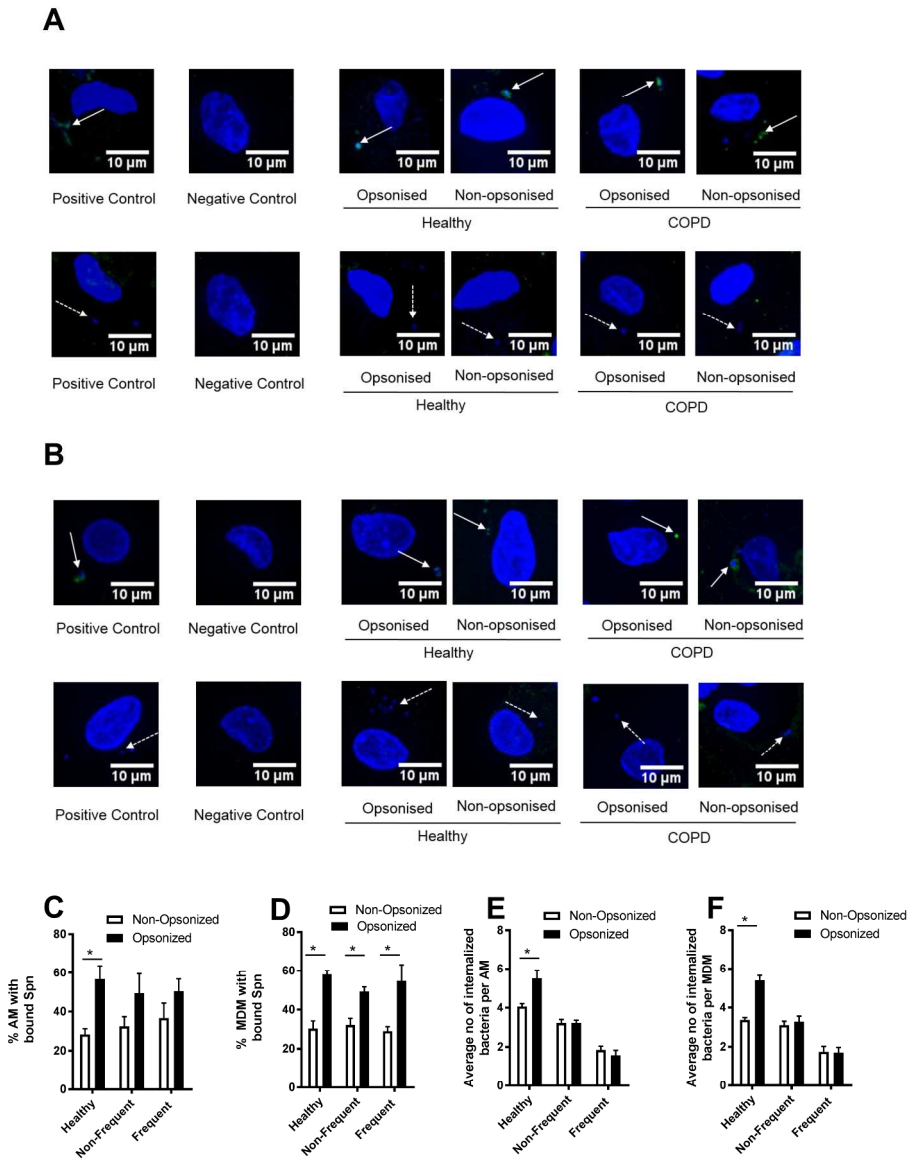

Figure E3. COPD alveolar macrophages show defects in uptake of opsonized S. pneumoniae. Alveolar macrophages (AM) or monocyte derived macrophages (MDM) were collected from patients with COPD or healthy donors and were challenged with non-opsonized or opsonized serotype 14 S. pneumoniae for 4h, before performing fluorescence microscopy to determine adherent (green, continuous arrows) and internalized bacteria (blue, broken arrows. Representative images are shown for fluorescence microscopy of AM (A) and MDM (B) with binding shown in the upper row and internalization in the lower row. In these experiments incubation on ice was a positive control for binding, IgG1 treatment to block Fc R was a negative control for both binding and internalization and treatment with 20% immune serum was a positive control for internalization. Pictures are representative of three donors in each condition. (C-F) AM (C and E) and MDM (D and F) from healthy and COPD donors (non-frequent or frequent exacerbators) were analyzed to record bacterial binding and internalization under the same conditions by fluorescence microscopy, n=4. * $p<0.05$ by One-way ANOVA.

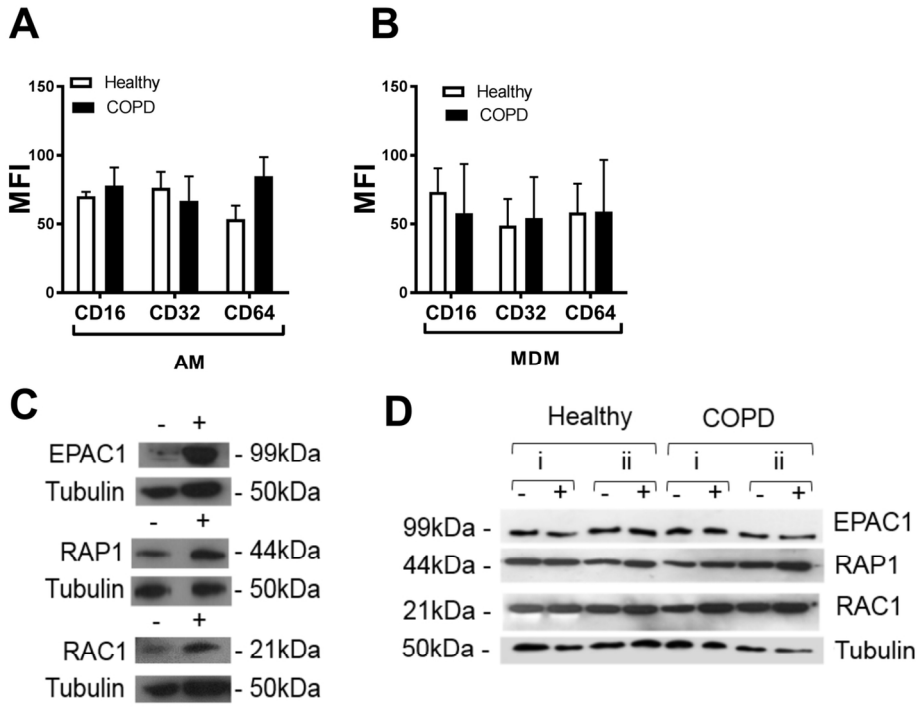

Figure E4. COPD Macrophages show no defect in Fc-gamma expression or expression of EPAC-1 RAP-1 and RAC-1.

(A-B) Healthy and COPD alveolar macrophages (AM) AM (A) and monocyte derived macrophages (MDM) (B) were analyzed for the expression of either CD16, CD32 or CD64 by flow cytometry, n=3, no significant differences between healthy or COPD. (C-D) Healthy or COPD AM from two individual donors (i and ii) were either mock-infected (Spn-) or challenged with serotype 14 S. pneumoniae (Spn +). 4h post-challenge cells were lysed and the expression of EPAC-1, RAP1 and RAC1 assessed by western blot. The blot is representative of one of three. (C) Positive controls (+) for EPAC-1, RAP-1 and RAC-1 were hypoxic MDM (as compared to nomoxic MDM (-)).

123x95mm (300 x 300 DPI)

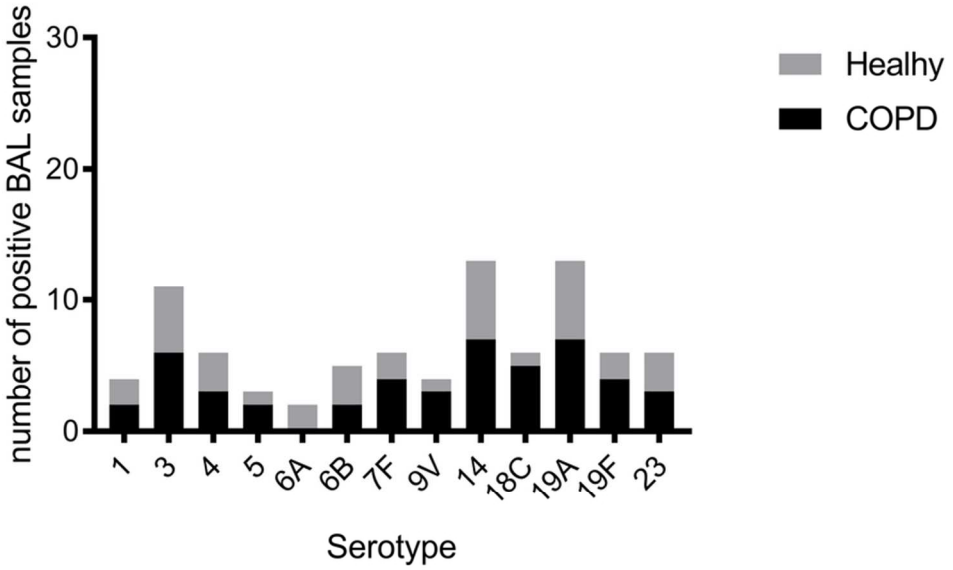

Figure E5 Pneumococcal antibodies are detectable in broncholaveolar lavage fluid. Bronchoalveolar lavage fluid from 13 healthy and 16 COPD patients was analyzed by multiplex immunoassay for presence of pneumococcal antibodies against 13 S. pneumoniae serotypes.

79x49mm (300 x 300 DPI)

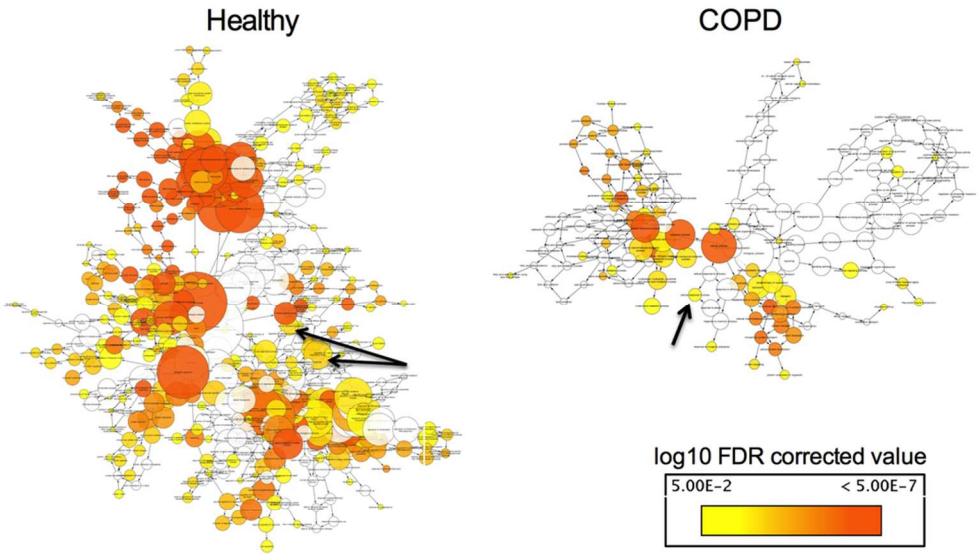

Figure E6. Transcriptional response of AM reveals less differential gene expression in COPD in response to infection. Ontology analysis of Healthy and COPD networks following pneumococcal challenge. The overrepresented terms (calculated with BiNGO software in Cytoscape, FDR <0.05, Hypergeometric clustering) are visualised. The terms for Cellular Response to Stress are highlighted by an arrow in each network.

95x59mm (300 x 300 DPI)

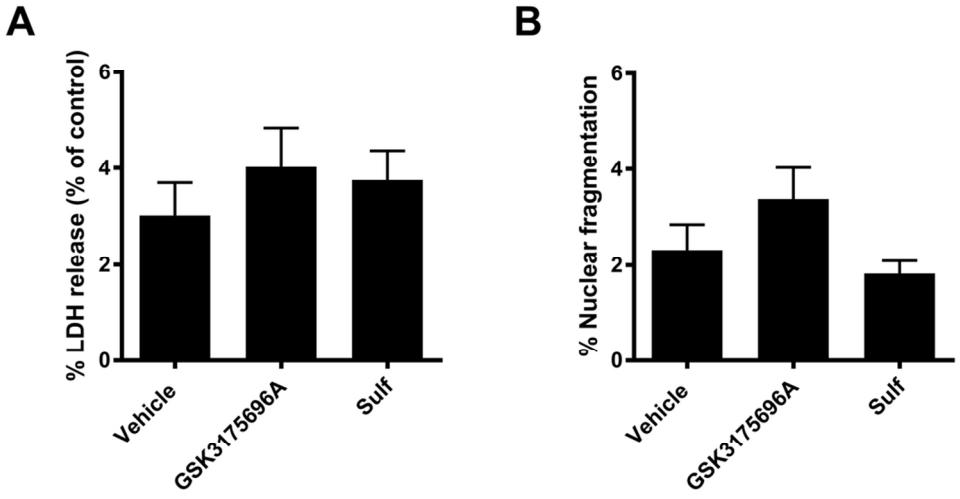

Figure E7. Treatment with Nrf-2 agonists does not induce apoptosis or necrosis. COPD alveolar macrophages were pre-treated with sulforaphane (+Sulf) or compound 7 for 16h. Cells were then assessed for either necrosis (A) or apoptosis (n=3).

98x54mm (300 x 300 DPI)

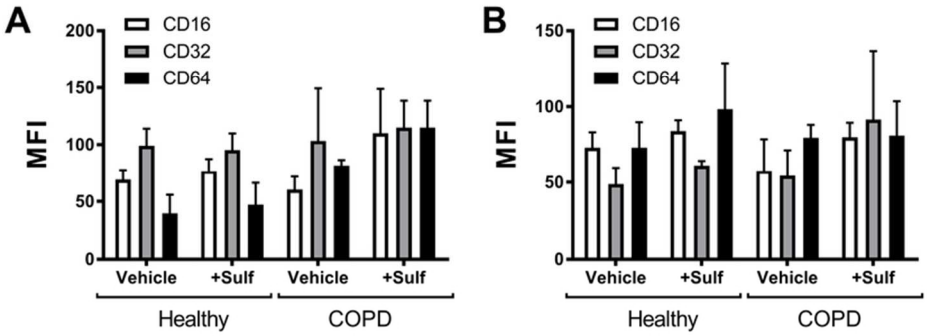

Figure E8. Sulforaphane treatment does not modify Fc-gamma expression in healthy or COPD macrophages. Healthy or COPD alveolar macrophages (AM)(A) or monocyte-derived macrophages (MDM)(B) were pre-treated with sulforaphane (+Sulf) for 16h. Cells were then assessed for expression of CD16, CD32 or CD64 by flow cytometry, n=3.

75x29mm (300 x 300 DPI)